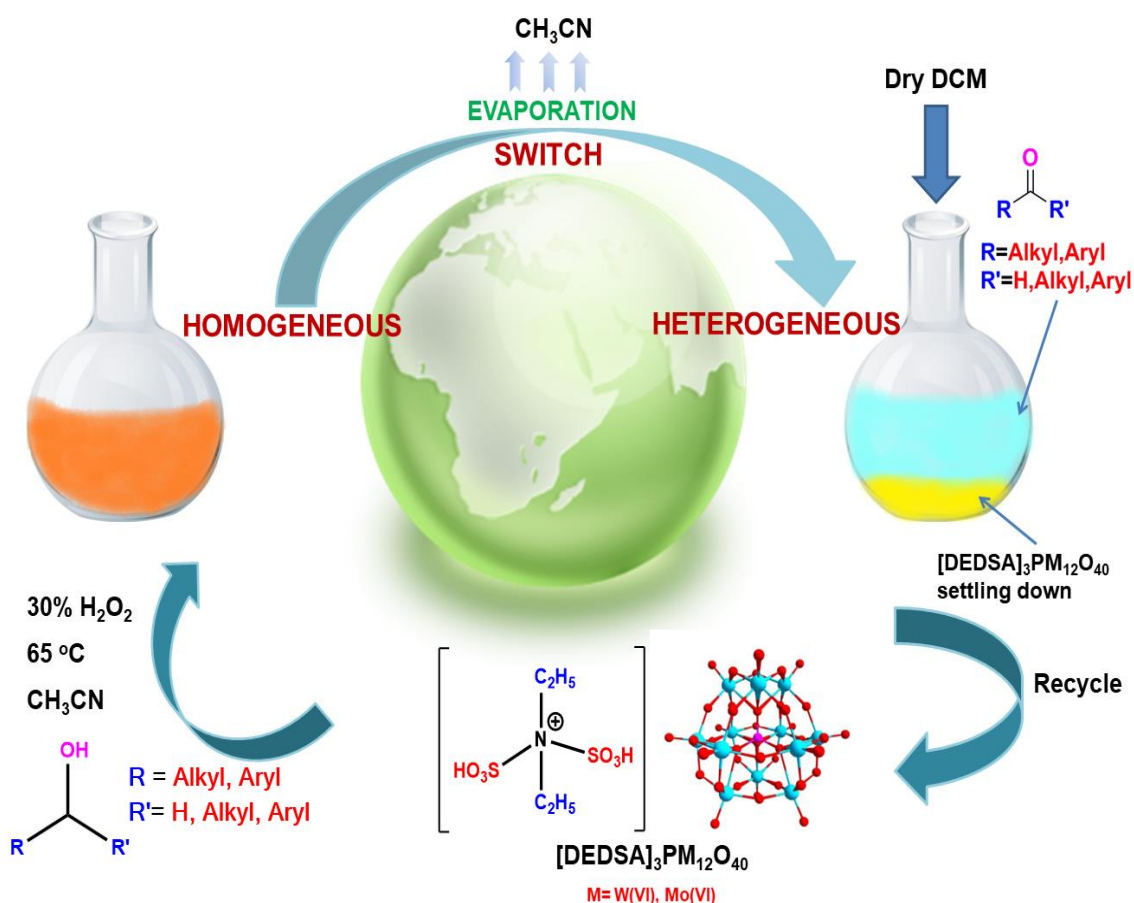


## Chapter-2

# Solvent responsive self-separative behaviour of Brønsted acidic ionic liquid-polyoxometalate hybrid catalysts on $\text{H}_2\text{O}_2$ mediated oxidation of alcohols



---

**Synopsis:** The solvent responsive self-separative behaviour of  $-\text{SO}_3\text{H}$  functionalized ionic liquid-based polyoxometalate catalyst through homogeneous and heterogeneous switching provides a facile way of alcohol oxidation in presence of benign oxidant  $\text{H}_2\text{O}_2$ . The recyclable organic-inorganic IL-POM based hybrid catalysts with high activity, high thermal stability combined with the advantages of both homogeneous and heterogeneous switching ability makes it suitable catalysts obliging the standards of environmental-friendly sustainable transformation.

Part of this chapter has been published in *Polyhedron*, 196, p.114993, 2021.

## 2.1. Introduction

Oxidation of primary and secondary alcohols to carbonyl compounds are being recognized as fundamental essentials for laboratories, pharmaceuticals, and other chemical manufacturing industries due to their vital role in organic synthesis [1-3]. Many conventional  $\text{CrO}_3$  and  $\text{K}_2\text{Cr}_2\text{O}_7$  based oxidant in acidic medium produce over oxidation product of primary alcohol i.e.  $-\text{COOH}$  from intermediate aldehyde which remains a problem in addition to stoichiometric amounts of oxidants, organic solvents, restriction for acid sensitive substrates, release of toxic reagents and inorganic side products to the environment [4-6]. Accompanied by the above mentioned various environmental issues, efforts have been made to produce reasonable oxidation protocols using environmentally benign oxidants having high active oxygen content and producing water as only byproduct at best [7,8]. As we have already discussed about polyoxometalates and its types in **Chapter-1A**, (section **1A.3**), so here we have explored structurally diverse combination of stable Keggin type metal-oxygen anionic clusters of early transition metals ( $\text{M}=\text{Mo}, \text{W}$ ) at their higher oxidation states in presence of heteroatom ( $\text{X} = \text{P}$ ) in producing a protocol for oxidation of alcohol in mild conditions [9]. The wide variation of composition, shapes, sizes, and charge densities provide numerous properties which led to exploration of these materials in catalysis, medicine, materials science, nanotechnology, molecular magnetism etc. [10-20].

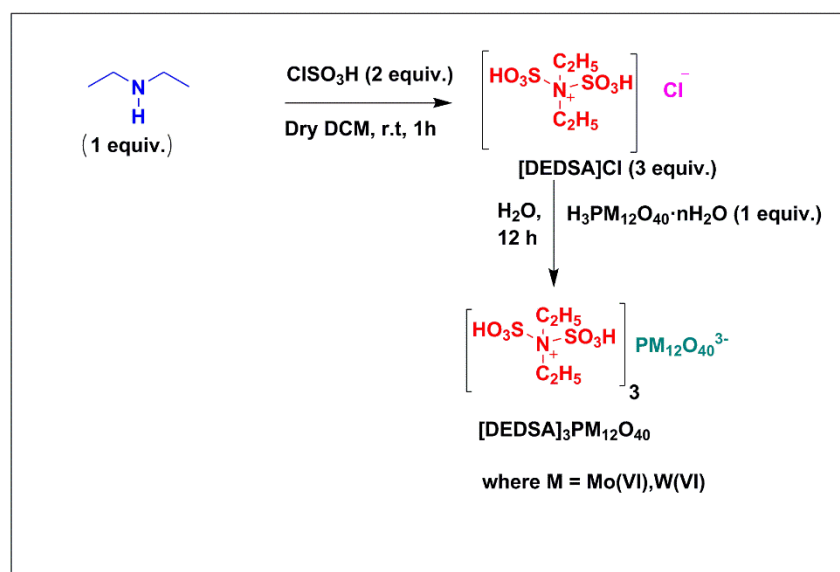
Polyoxometalates show excellent multi-electron redox cycles without major change of their structures in homogeneous or heterogeneous phases [21-27]. Moreover, they are less toxic as compared to the chromate-based oxidant. The solubility of POMs in

polar solvent increases their activity as redox catalysts for the oxidation of alcohol using  $\text{H}_2\text{O}_2$  as oxidant in homogeneous phase [11, 12, 28]. The recyclability limitation of homogeneous POMs was solved through heterogenization of the POMs on inert support with high surface area materials. But these supported catalysts also showed slow reaction rates for aggregation and leaching from the support due to weaker binding interaction between them [16]. Consequently, many organic–inorganic hybrid POMs were designed to effectively deal with the problems faced by the POM catalytic systems with modification of their characteristic structural nature like high thermal stability, rich redox properties have been isolated [24-27].

Ionic liquids (ILs) have been used extensively for designing task-specific catalysts, used as reaction media, and also functionalized solvent because of their unique physical properties such as wider range of melting points to be in liquid state, high thermal stability, viscous nature, appropriate solvation behavior etc. [29]. The presence of organic cation into the POM framework increases the porosity of the structure and modify their polarity through hydrophobic interaction which may work as controlling factor for varied solvent responsive behaviour of the hybrid depending on the nature of organic cation. These modifications of the POM structures may facilitate them as a new type of POM-based catalysts having great potential in heterogeneous catalysis. The variation of organic cations in to the POMs provides an efficient approach to synthesize multifunctional materials based on the nature of organic part in molecular level [30]. Task-specific (TSILs) ionic liquids are an important group of ionic liquids with growing applications in synthesis, catalysis, electrochemistry etc. in which functional groups are covalently tethered to the cation or anion or both the ions [31]. Brönsted acidic ionic liquids were designed by tethering acid groups to the ILs and this type of TSILs along with providing acidic functionality to acid catalyzed reactions also helps in avoiding strong mineral acids with volatile harmful acid vapors [32]. Similarly basic TSILs are also designed and were investigated for various applications [33, 34]. Ion-pairing of organic cation with the POM anion generates new type of ionic liquid-based hybrid POMs (IL-POMs) as stable solid acidic material with high melting points that can be utilized as heterogeneous catalyst [35,36].

Modification of the POMs by incorporation of organic moiety has improved the catalytic activity as well as recovery and reusability related issues. Till date several IL-

POM hybrids have been studied for base catalyzed reactions, acid catalyzed reactions, oxidation reactions etc. with unique self-separation properties as catalysts based on light sensitivity, temperature variation and other stimuli responsive [35-41]. Literature review on use of various ionic-liquid polyoxometalate hybrids have already been stated in **Chapter 1A**, (section **1A.6**). Here our main aim was to design hybrids which can act as phase transfer catalyst with the advantage of being switchable homogeneous and heterogeneous property in response to additive solvent. In this context, we decided to design N-SO<sub>3</sub>H functionalized diethyldisulfoammonium based Keggin POMs with sulfonic groups and hydrophobic groups like ethyl for working as solvent-responsive self-separation catalyst through variation of interactions with different solvents. The scheme of synthesis of organic-inorganic IL-POM based hybrids is provided in (**Scheme 2.1**). These two hybrids were explored as recyclable self-separative catalysts for oxidation of alcohols using 30% H<sub>2</sub>O<sub>2</sub> as green oxidant at 65 °C after characterization with various analytical techniques.



**Scheme 2.1:** Synthesis of [DEDSA]<sub>3</sub>PM<sub>12</sub>O<sub>40</sub>.

## 2.2. Results and discussion

The preparation of diethyldisulfoammonium salts of Keggin anions [DEDSA]<sub>3</sub>[PM<sub>12</sub>O<sub>40</sub>] where M= Mo (VI), W(VI) were carried out in two step method (**Scheme 2.1**) as mentioned in the experimental section **2.5**. The pure organic-inorganic IL-POM based

hybrid salts were analyzed by different analytical techniques for structural confirmations, thermal stability study. The redox properties of the organic-inorganic IL-POM based hybrids were investigated as solvent responsive self- separation catalyst for selective oxidation of benzylic alcohol to aldehyde and secondary alcohol to keto compound.

### 2.2.1 FT-IR analysis

The existence of Keggin structures of heteropolyanions in the organic-inorganic IL-POM based hybrids were confirmed by comparing their characteristic peaks with the IR spectra of heteropolyacids (HPAs) in **Fig. 2.1(a) & 2.1(b)**. It is well defined that  $\alpha$ -Keggin anion is a combination of a  $[XO_4]$  tetrahedron of P or Si and  $[MO_6]$  octahedra. The  $[MO_6]$  octahedral units are edge shared into four  $C_{3v}$   $[M_3O_{13}]$  groups and are connected to the three-fold axes of the central  $[XO_4]$  tetrahedron. The metal atoms are situated at the centres of distorted  $C_s$  octahedra with one terminal  $M-O_t$  bond. The  $M-O_{4c}$  bonds attributes four-coordinate oxygen atoms that connects 3 units of  $[MO_6]$  and  $[XO_4]$  unit. The  $M-O_{2c1}$  bonds and  $Mo-O_{2c2}$  bonds attributes two-coordinate oxygen atoms in which the  $M-O_{2c1}$  bonds connects the  $[MO_6]$  octahedra into  $[M_3O_{13}]$  groups whereas the  $M-O_{2c2}$  bonds connect the  $[M_3O_{13}]$  units together [42]. Herein, both the POM hybrids displayed peaks correspond to P-O bending ( $593\text{ cm}^{-1}$ ), asymmetric stretch of  $M-O_{2c2}$ -M bonds involving edge sharing  $MO_6$  octahedra ( $714\text{-}810\text{ cm}^{-1}$ ), asymmetric stretch of  $M-O_{2c2}$ -M bonds of corner  $MO_6$  octahedra ( $866\text{-}898\text{ cm}^{-1}$ ), asymmetric  $M-O_t$  stretch ( $960\text{-}990\text{ cm}^{-1}$ ), asymmetric P-O stretch ( $1049\text{-}1097\text{ cm}^{-1}$ ) and bending vibrations of water molecules in the secondary structures of the Keggin species ( $1623\text{-}1628\text{ cm}^{-1}$ ). The tethering of  $-SO_3H$  groups to the diethyldisulfoammonium cation can be attributed from antisymmetric S-O stretch ( $1147\text{-}1166\text{ cm}^{-1}$ ), overlapping bands of symmetric S-O stretch with the asymmetric P-O stretch and N-S stretch with the asymmetric stretch of  $M-O_{2c2}$ -M bonds of corner  $MO_6$  octahedra were observed. Very weak band of C-N stretch for aliphatic amine at around ( $1020\text{-}1250\text{ cm}^{-1}$ ) was observed. The two ethyl groups directly attached to the ammonium cation also showed C-H rocking ( $1350\text{-}1392\text{ cm}^{-1}$ ), C-H bending ( $1450\text{-}1470\text{ cm}^{-1}$ ) and C-H stretching vibrations ( $2844, 2943 \& 3091\text{-}3109\text{ cm}^{-1}$ ) in the respective IR spectra of the organic-inorganic IL-POM based hybrids [40, 42-45].

A weak intensity broad band at  $3433\text{ cm}^{-1}$  compared to the heteropolyacids indicates minimum amount of strongly H-bonded water molecules in rigid framework of phosphomolybdate anion and phosphotungstate anion along with -OH bond of sulfonic groups. The reduction in broadening of the O-H band above  $3000\text{ cm}^{-1}$  in the POM hybrids

justifies the presence of smaller hydration sphere around the heteropolyanion environment which is also observed in case of deshielding in the resonance peaks in the respective  $^{31}\text{P}$  NMR spectra of the hybrids [46].

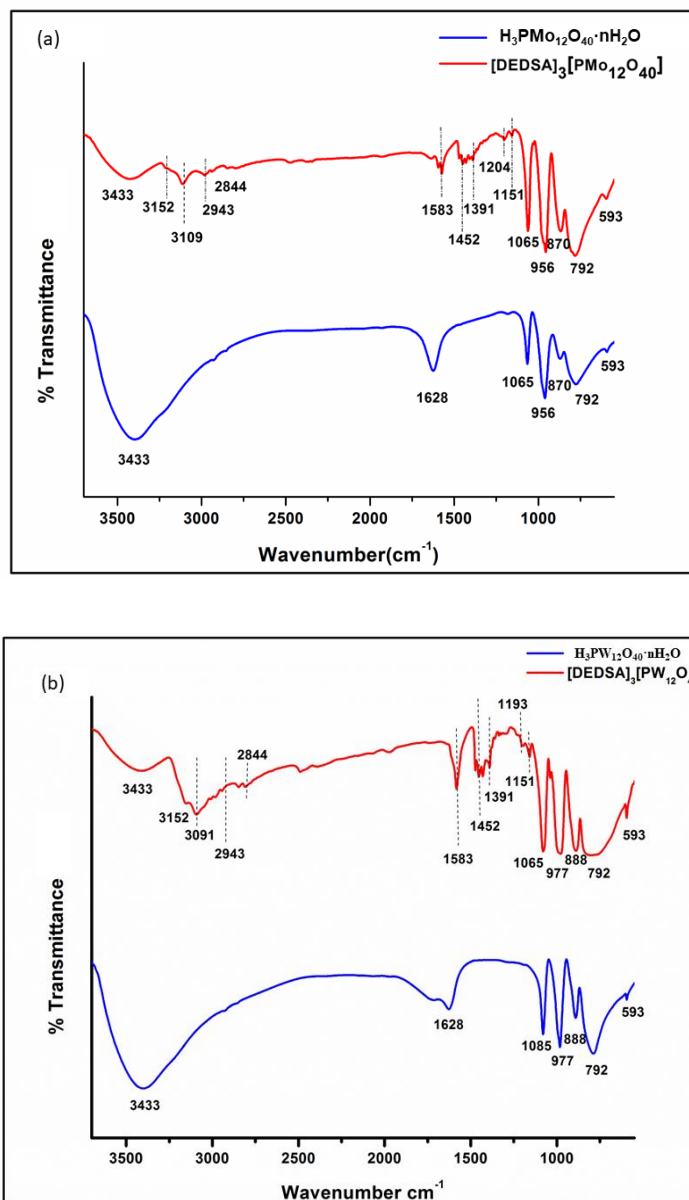


**Fig. 2.1:** FT-IR spectra of (a)  $\text{H}_3\text{PMO}_{12}\text{O}_{40}\cdot n\text{H}_2\text{O}$  and  $[\text{DEDSA}]_3[\text{PMO}_{12}\text{O}_{40}]$  and (b)  $\text{H}_3\text{PW}_{12}\text{O}_{40}\cdot n\text{H}_2\text{O}$  and  $[\text{DEDSA}]_3[\text{PW}_{12}\text{O}_{40}]$  respectively.

### 2.2.2 NMR analysis

Proton NMR analysis of the  $[\text{DEDSA}]_3[\text{PMO}_{12}\text{O}_{40}]$  and  $[\text{DEDSA}]_3[\text{PW}_{12}\text{O}_{40}]$  in  $\text{DMSO}-d_6$  displayed two  $-\text{CH}_3$  groups as triplet at 1.12 ppm, two methylene groups as quartet at 2.87 ppm and one broad singlet for two  $-\text{SO}_3\text{H}$  protons at 8.14-8.15 ppm (**Fig. 2.2a and 2.2b**)

respectively. The  $^{13}\text{C}$  NMR of these POM hybrids showed two peaks at 41.83-42.1 ppm and 11.6 ppm corresponding to ethyl groups of ammonium cation (**Fig. 2.3a and 2.3b**). The  $^{31}\text{P}$  NMR spectrum of  $[\text{DEDSA}]_3[\text{PMo}_{12}\text{O}_{40}]$  hybrid salt expressed one peak at -3.65 ppm (**Fig. 2.4a**) which was observed in higher frequency region compared to -3.51 ppm

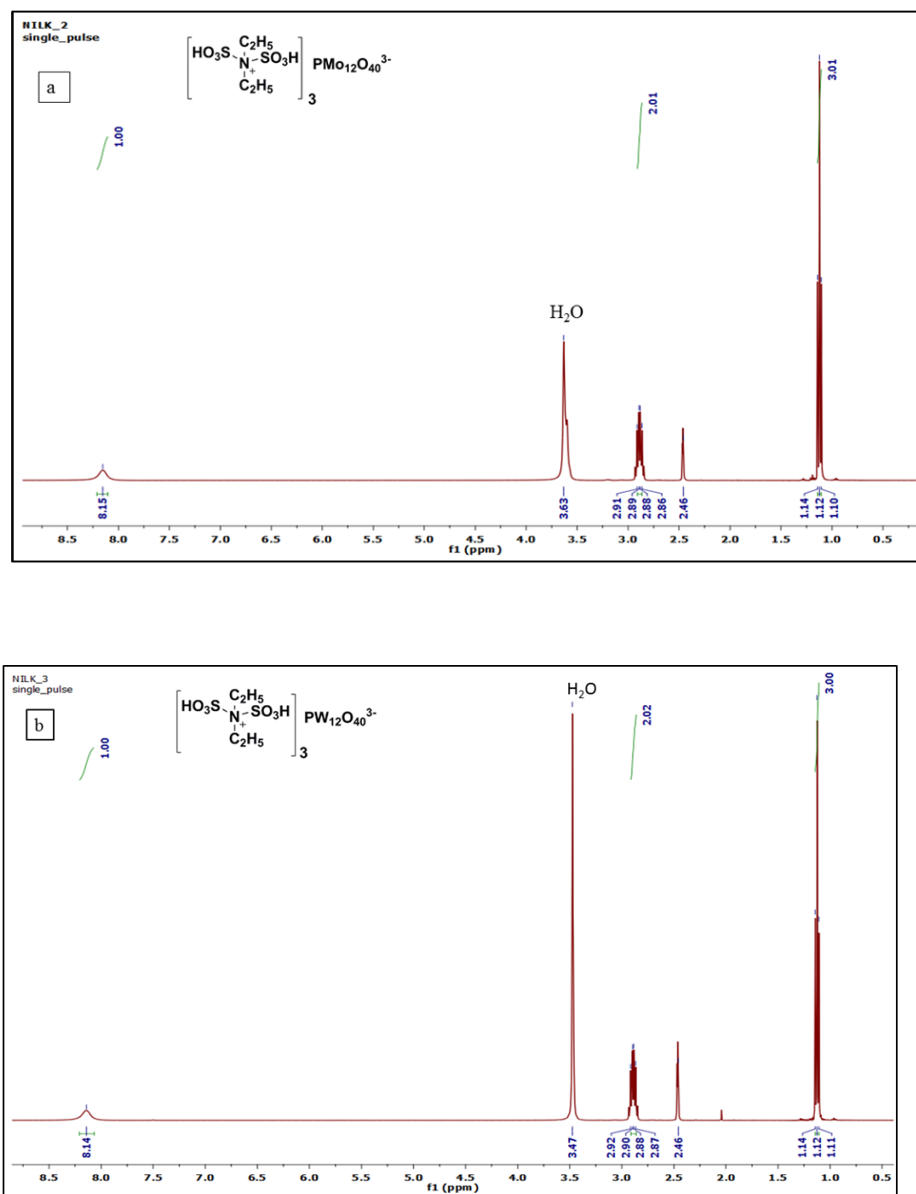


**Fig. 2.2:**  $^1\text{H}$  NMR spectra of (a)  $[\text{DEDSA}]_3[\text{PMo}_{12}\text{O}_{40}]$  and (b)  $[\text{DEDSA}]_3[\text{PW}_{12}\text{O}_{40}]$ .

peak of the phosphomolybdic acid (**Fig. 2.5a**). In case of  $[\text{DEDSA}]_3\text{PW}_{12}\text{O}_{40}$  there is similar kind of frequency shift of the hybrid to -15.15 ppm is observed (**Fig. 2.4b**) whereas

a single peak appeared at -14.72 for the phosphotungstic acid (**Fig. 2.5b**) indicating strong ionic interaction between the organic cation and the Keggin anion. The shift in the resonance peaks in  $^{31}\text{P}$  indicates dehydration in the organic-inorganic IL-POM based hybrids which ascribes the presence of smaller hydration sphere in the polyanion environment noticed for dynamic dehydration equilibrium [ 47,48].

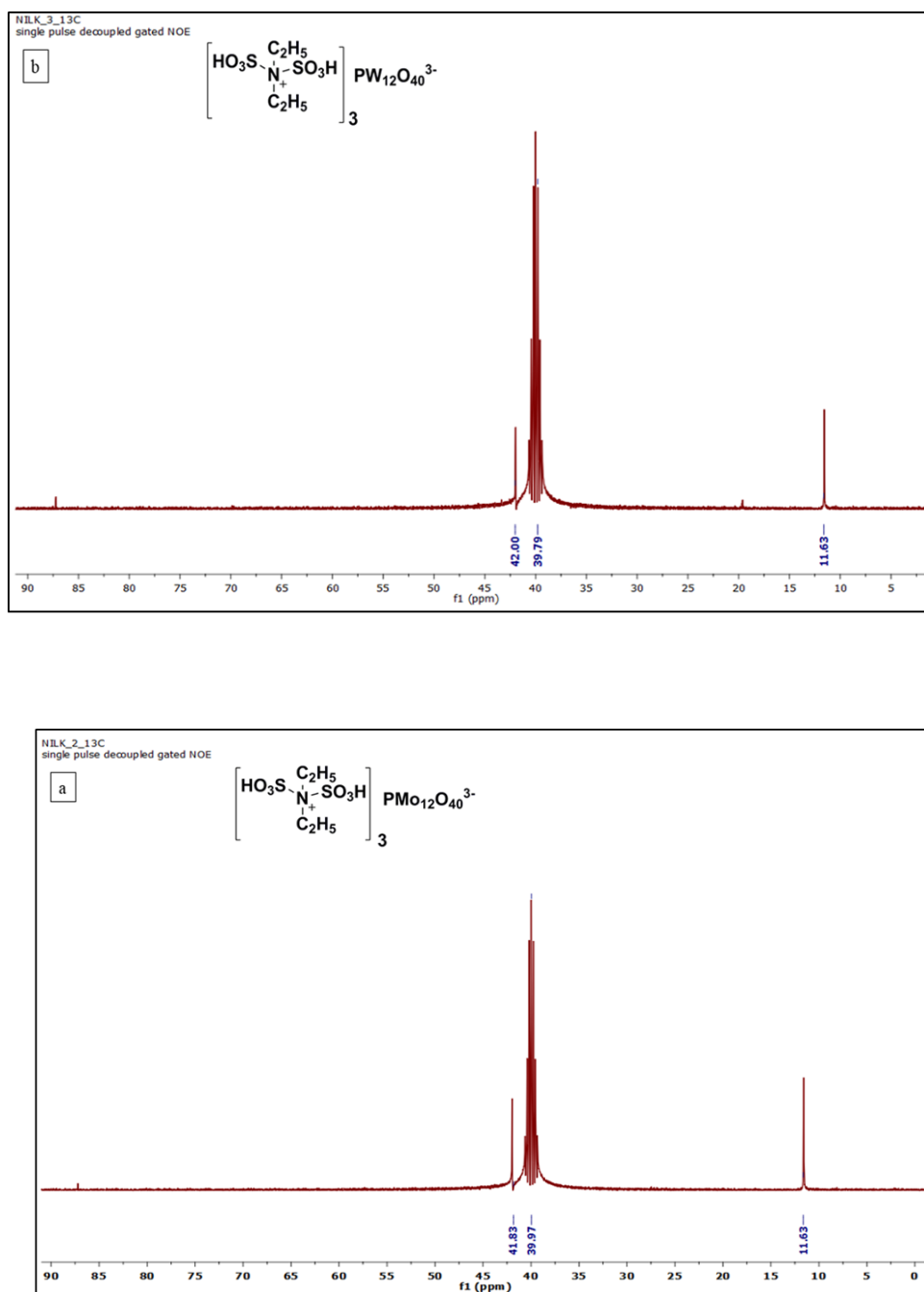


**Fig. 2.3:**  $^{13}\text{C}$  NMR spectra of (a) [DEDSA] $_3$ [PMo $_{12}$ O $_{40}$ ] $^{3-}$  and (b) [DEDSA] $_3$ [PW $_{12}$ O $_{40}$ ] $^{3-}$ .



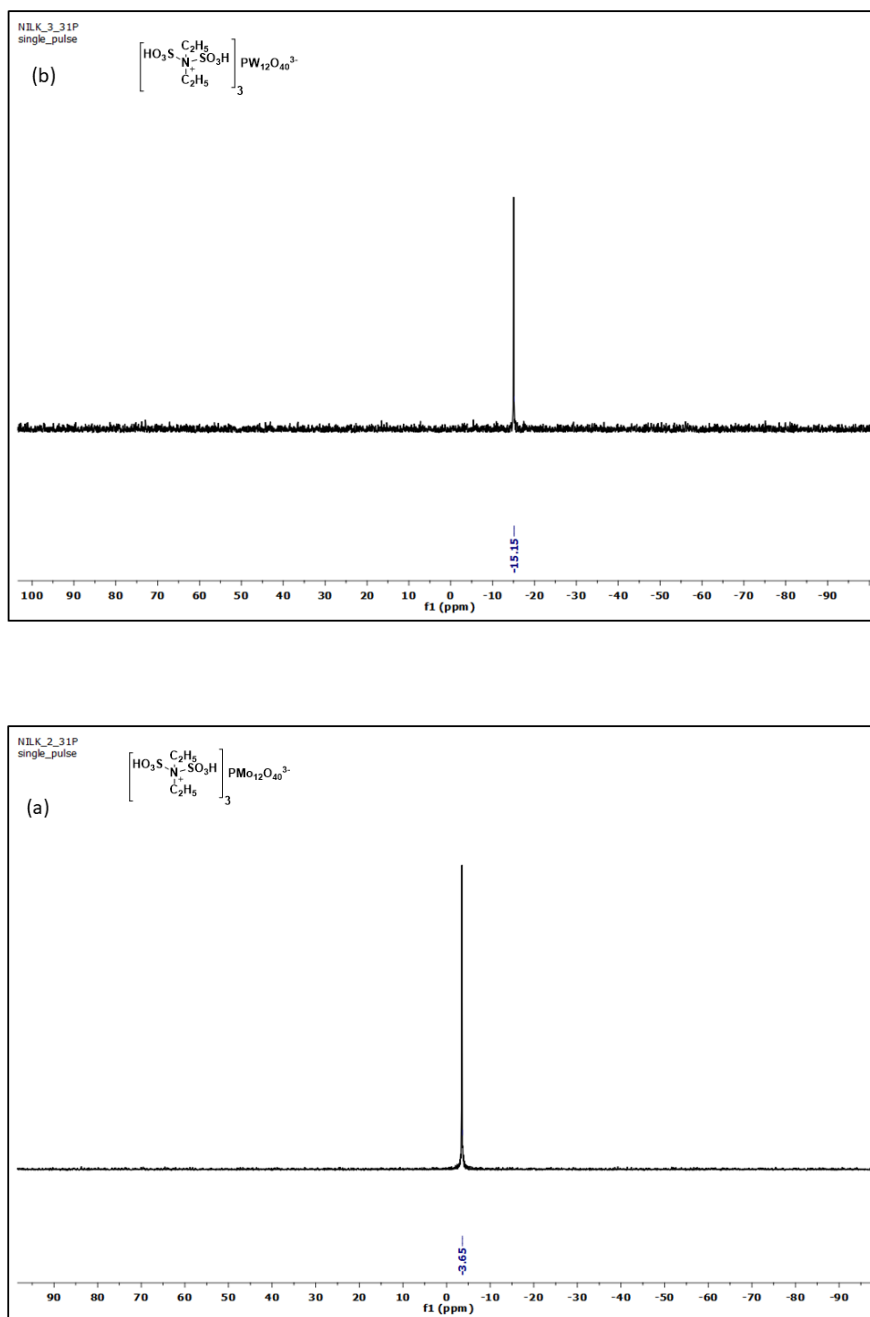


**Fig. 2.4:**  $^{31}\text{P}$  NMR spectra of (a)  $[\text{DEDSA}]_3[\text{PMO}_{12}\text{O}_{40}]$  and (b)  $[\text{DEDSA}]_3[\text{PW}_{12}\text{O}_{40}]$ .

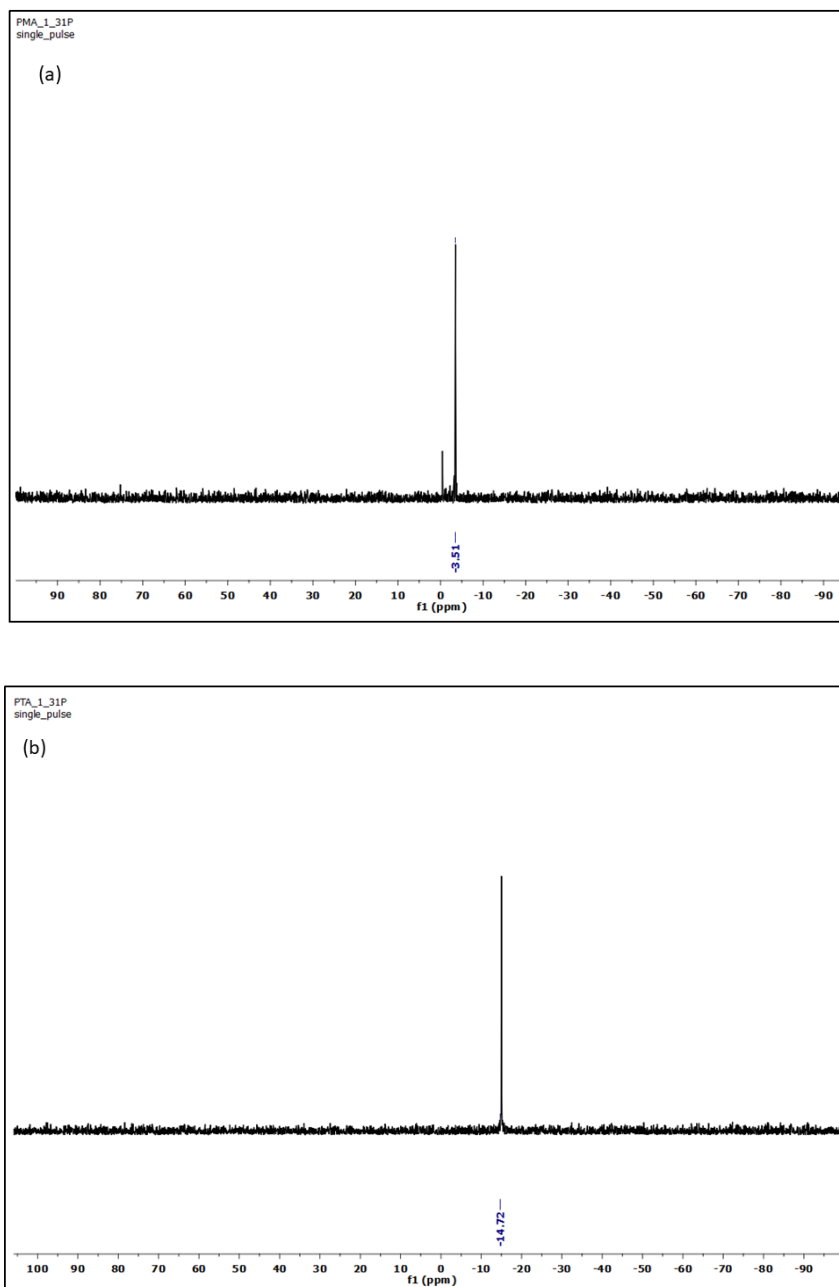


**Fig. 2.5:** <sup>31</sup>P NMR spectra of (a) H<sub>3</sub>PMo<sub>12</sub>O<sub>40</sub>·nH<sub>2</sub>O and (b) H<sub>3</sub>PW<sub>12</sub>O<sub>40</sub>·nH<sub>2</sub>O.

### 2.2.3 Elemental analysis

Elemental analysis of [DEDSA]Cl, [DEDSA]<sub>3</sub>[PMo<sub>12</sub>O<sub>40</sub>] and [DEDSA]<sub>3</sub>[PW<sub>12</sub>O<sub>40</sub>] were conducted using CHN analyser for percentage of C, H, N elements present in the parent ionic liquid and hybrids. The metal composition of the hybrids were analysed using ICP-OES following the method mentioned in Chapter 1B (section 1B.3.9). **Table 2.1** includes the ICP-OES data of the synthesized hybrids. However, the CHN analysis data of the parent ionic liquid is included in the spectral data section **Table 2.5**. The CHN analysis

results prove that three units of parent ionic liquid cation are bonded against one unit of polyoxometalate anion. Calculated for  $[\text{DEDSA}]_3\text{PMo}_{12}\text{O}_{40}$  (%): C 5.70, N 1.66, H 1.44 Found: C 5.88, N 1.72, H 1.37. Calculated for  $[\text{DEDSA}]_3\text{PW}_{12}\text{O}_{40}$  (%): C 4.02, N 1.17, H 1.01. Found: C 4.15, N 1.22, H 1.11.

**Table 2.1** ICP-OES analyses for metal content of the organic-inorganic IL-POM based hybrids

Entry	Sample	% of metal content
		Calculated (Found)
1.	$[\text{DEDSA}]_3[\text{PMo}_{12}\text{O}_{40}]$	Mo, 45.66 (46.12%)
2.	$[\text{DEDSA}]_3[\text{PW}_{12}\text{O}_{40}]$	W, 61.21% (62.01%)

## 2.2.4 TGA

Thermogravimetric analysis (TGA) showed absence of physisorbed water (**Fig. 2.6**) for the two organic-inorganic IL-POM based hybrids  $[\text{DEDSA}]_3[\text{PM}_{12}\text{O}_{40}]$  up to 100 °C as compared to approximately 13% loss of the physisorbed water in case of the precursor  $[\text{DEDSA}]\text{Cl}$  ionic liquid.

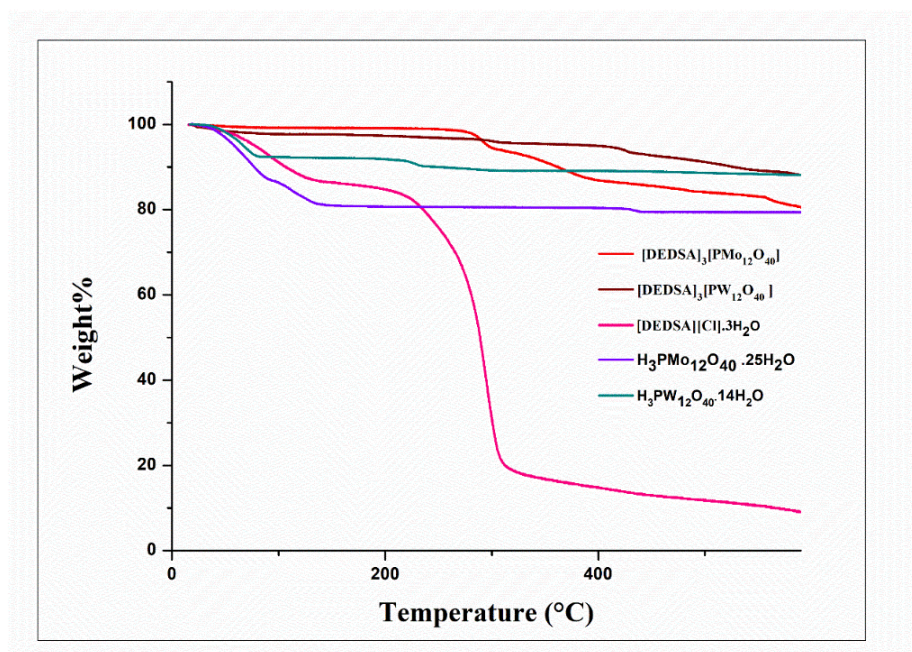


**Fig. 2.6:** TGA curves of  $[\text{DEDSA}]_3[\text{PW}_{12}\text{O}_{40}]$ ,  $[\text{DEDSA}]_3[\text{PMo}_{12}\text{O}_{40}]$ ,  $[\text{DEDSA}]\text{Cl} \cdot 3\text{H}_2\text{O}$ ,  $\text{H}_3\text{PMo}_{12}\text{O}_{40} \cdot 25\text{H}_2\text{O}$  and  $\text{H}_3\text{PW}_{12}\text{O}_{40} \cdot 14\text{H}_2\text{O}$ .

The chloride based ionic liquid expressed another degradation at 190 °C which can be expected for stepwise removal of the two  $-\text{SO}_3\text{H}$  group of the diethyldisulphoammonium moiety along with the degradation of the complete organic moiety. The TGA pattern of  $[\text{DEDSA}]_3[\text{PMo}_{12}\text{O}_{40}]$  displayed its thermal stability till 285 °C, whereas it was observed up to 412 °C for the  $[\text{DEDSA}]_3[\text{PW}_{12}\text{O}_{40}]$  with residue of the Keggin anions [49]. The least amount of physisorbed water in the POM hybrids can also be evidenced from the respective FT-IR spectra and  $^{31}\text{P}$  NMR.

### 2.2.5 Powder XRD analysis

The powder XRD patterns of both the POM-hybrid samples confirmed the presence of Keggin structures of  $[\text{PMo}_{12}\text{O}_{40}]^{3-}$  and  $[\text{PW}_{12}\text{O}_{40}]^{3-}$  in **Fig. 2.7**. Typical sharp diffraction peaks of the  $\text{H}_3\text{PMo}_{12}\text{O}_{40}\cdot n\text{H}_2\text{O}$  are observed at  $6.78^\circ$  and  $26.79^\circ$  [**Fig. 2.7**]. In case of  $[\text{DEDSA}]_3[\text{PMo}_{12}\text{O}_{40}]$ , additional peaks appeared at around  $8.5^\circ$  along with less intensity peak at  $6.76^\circ$ , while the other prominent peak of  $\text{H}_3\text{PMo}_{12}\text{O}_{40}\cdot n\text{H}_2\text{O}$  at  $26.79^\circ$  almost disappeared for the hybrid [**Fig. 2.7**]. Intense peak at  $6.79^\circ$  and  $8.55^\circ$  observed in the  $\text{H}_3\text{PW}_{12}\text{O}_{40}\cdot n\text{H}_2\text{O}$  reduced drastically in  $[\text{DEDSA}]_3[\text{PW}_{12}\text{O}_{40}]$  [**Fig. 2.7**]. In this hybrid, new peaks are found with lower intensity within  $2\theta$  values of  $11^\circ$ - $17^\circ$ . The disappearance of few sharp peaks and appearance of new peaks in the organic-inorganic IL-POM based hybrids as compared to their parent acids can be expected from reorganization of crystal structures of heteropolyacid in the organic-inorganic IL-POM based hybrids in presence of large organic cation due to deviation of planes in the crystal lattice involving self assembly of the Keggin anions and the organic cations via electrostatic force, hydrogen bonding etc. [46,50,51].

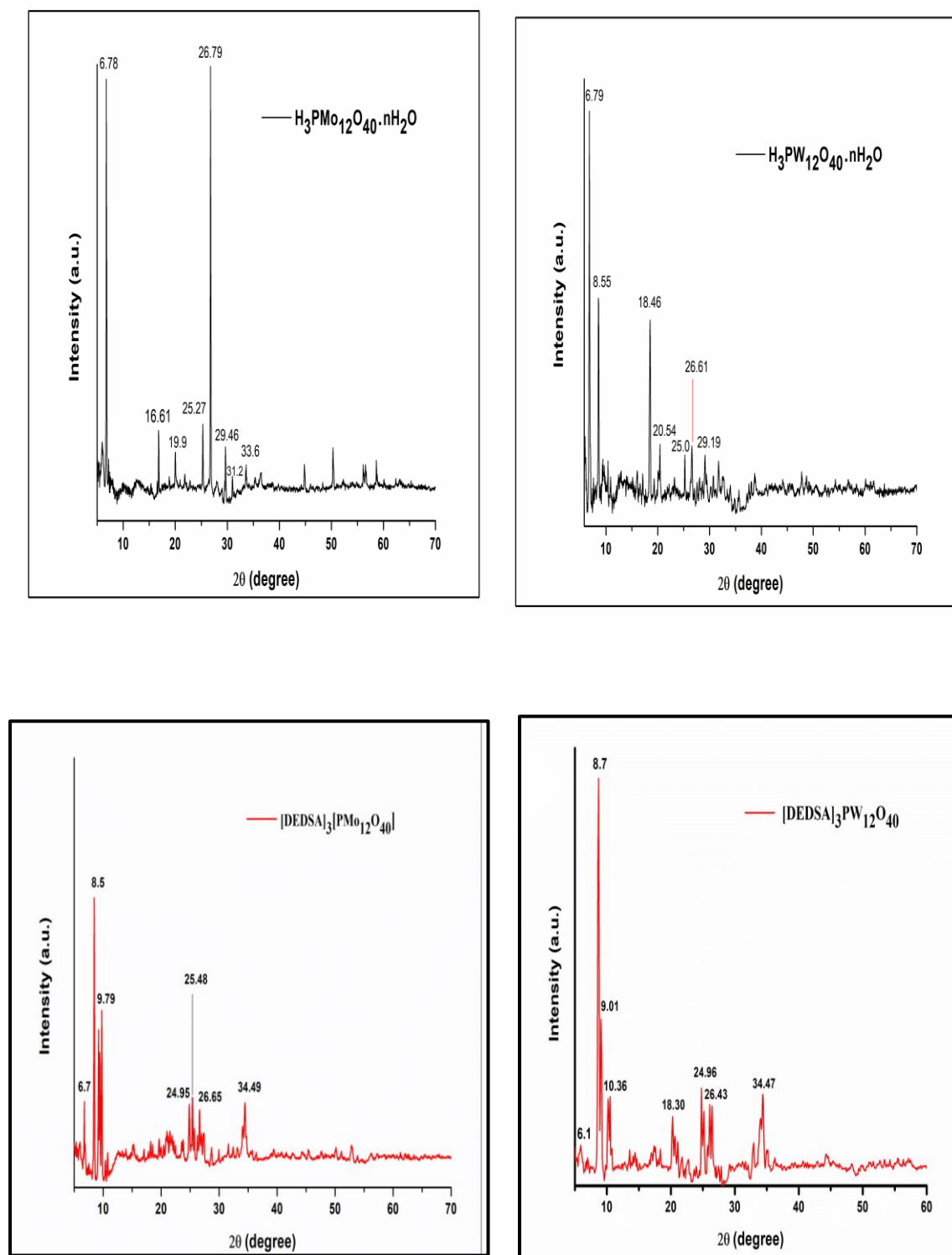
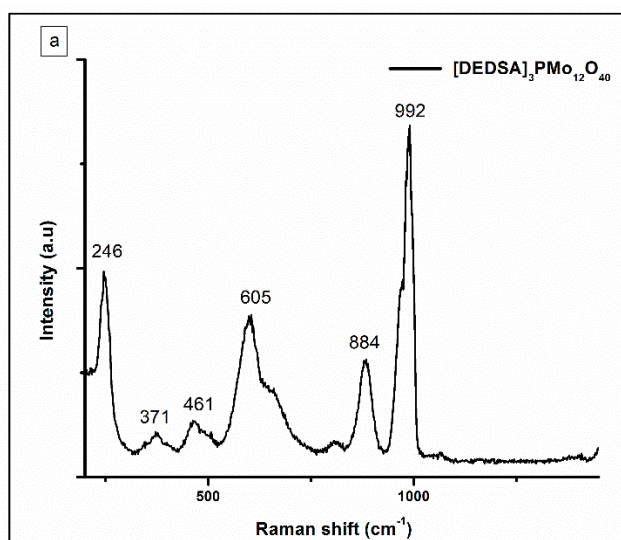


**Fig. 2.7:** Powder XRD analysis patterns of (a)  $[\text{DEDSA}]_3[\text{PMo}_{12}\text{O}_{40}]$  and  $\text{H}_3\text{PMo}_{12}\text{O}_{40} \cdot n\text{H}_2\text{O}$  (b)  $[\text{DEDSA}]_3[\text{PW}_{12}\text{O}_{40}]$  and  $\text{H}_3\text{PW}_{12}\text{O}_{40} \cdot n\text{H}_2\text{O}$ .

## 2.2.6 Raman analysis

Raman spectra of the hybrids in **Fig. 2.8 (a)** and **(b)** showed resemblance of characteristic bands of the Keggin anions  $[\text{PMo}_{12}\text{O}_{40}]^{3-}$  and  $[\text{PW}_{12}\text{O}_{40}]^{3-}$  observed from Bridgeman's assignments [42,52]. A very sharp-edged peak at  $992\text{ cm}^{-1}$  for the phosphomolybdate hybrid is observed for symmetric stretch of  $\text{Mo-O}_t$  bond. Another peak at  $884\text{ cm}^{-1}$  is assigned for asymmetric stretch of  $\text{Mo-O}_{2c2}$ -Mo bonds. Combined stretching and bending vibrations of  $\text{Mo-O}_{2c1}$ -Mo bonds could be attributed to medium intensity broad shoulder at  $605\text{ cm}^{-1}$ . The small intensity sharp peak at  $246\text{ cm}^{-1}$  is accounted for overlapping symmetric stretch of  $\text{Mo-O}_{4c}$  and bending of the intra ligand  $\text{Mo-O}_{2c2}$ -O bond. Remaining few very weak Raman bands are related to complex Raman modes of the polyoxometalate anion.

Similarly, in case of the  $[\text{DEDSA}]_3[\text{PW}_{12}\text{O}_{40}]$ , a very sharp band at  $1002\text{ cm}^{-1}$  is assigned to the symmetric stretch of terminal  $\text{W-O}_t$  bond. The medium intense band at  $910\text{ cm}^{-1}$  is observed for asymmetric stretch of  $\text{W-O}_{2c2}$ -W bond. A very weak intensity peaks is observed at  $664\text{ cm}^{-1}$  which could be considered for combined stretching and bending vibrations of  $\text{W-O}_{2c1}$ -W bond. The weak band at  $226\text{ cm}^{-1}$  could be allotted for  $\text{W-O}_{4c}$  symmetric stretching vibrations.



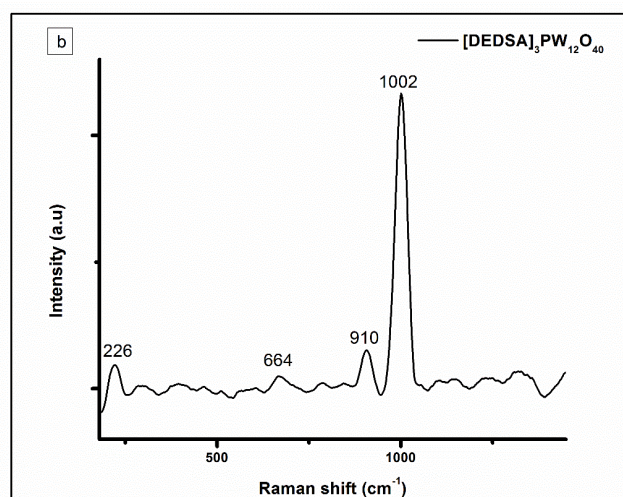


**Fig. 2.8:** Raman spectra of (a) [DEDSA]<sub>3</sub>[PMo<sub>12</sub>O<sub>40</sub>] and (b) [DEDSA]<sub>3</sub>[PW<sub>12</sub>O<sub>40</sub>].

### 2.2.7 UV-Vis diffuse reflectance spectroscopy analysis

The UV-Vis diffuse reflectance spectra of the organic-inorganic IL-POM based hybrids and the HPAs are represented in **Fig. 2.9 (a) & (b)**. The retention of Keggin structures [PM<sub>12</sub>O<sub>40</sub>]<sup>3-</sup> (M= W or Mo) within the hybrid compounds can be supported from their UV-Vis DRS absorption patterns against the respective HPAs. The weak intensity peaks of phosphotungstate Keggin anion at 259, 347 and 402 nm expressed oxygen to metal charge transfer transition (LMCT) for non-reduced form of the HPA Keggin anion [53], **Fig. 2.9b**. Similarly, for the Keggin anion of the phosphomolybdic acid displayed the weaker LMCT transitions at 218, 347 and 455 nm in **Fig. 2.9a** [54]. As compared to the HPAs, the Keggin anions of the POM-hybrid samples shifted the position of LMCT transitions to shorter wavelength which indirectly reflect the existence of strong ionic interaction between the constituent ion-pairs [54]. For example, the highest absorption peak of the HPA of phosphotungstate anion shifted from 402 nm to 339 nm in the [DEDSA]<sub>3</sub>[PW<sub>12</sub>O<sub>40</sub>] hybrid. Likely, with the [DEDSA]<sub>3</sub>[PMo<sub>12</sub>O<sub>40</sub>], it was shifted to 396 nm from 455 nm.

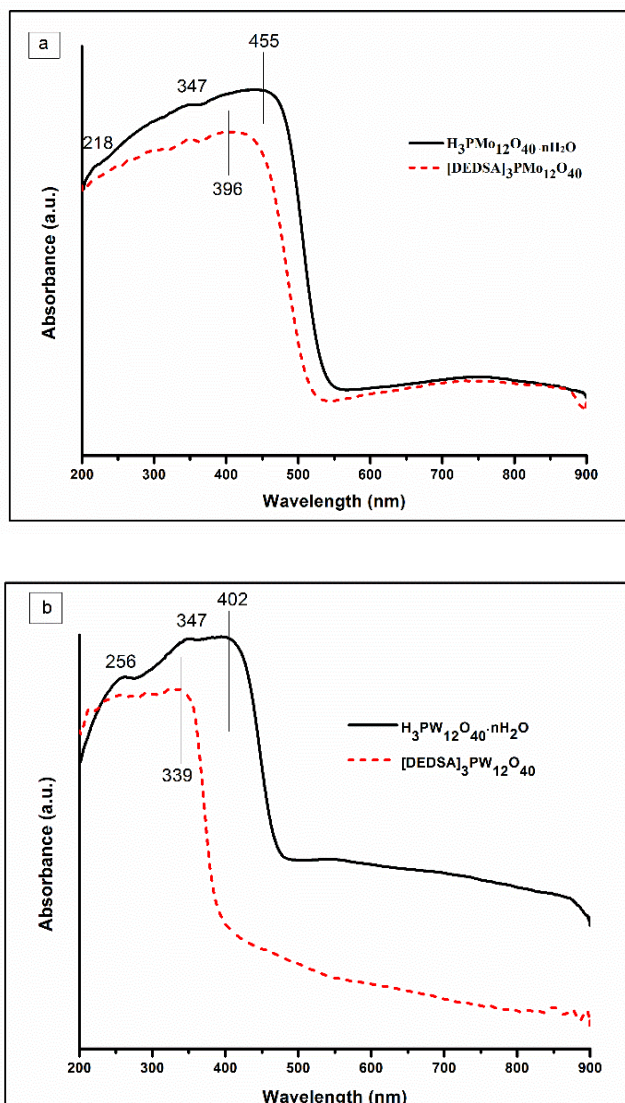


**Fig. 2.9:** UV-Vis DRS spectra of (a)  $[\text{DEDSA}]_3[\text{PMO}_{12}\text{O}_{40}]$  and  $\text{H}_3\text{PMO}_{12}\text{O}_{40} \cdot n\text{H}_2\text{O}$  (b)  $[\text{DEDSA}]_3[\text{PW}_{12}\text{O}_{40}]$  and  $\text{H}_3\text{PW}_{12}\text{O}_{40} \cdot n\text{H}_2\text{O}$ .

### 2.2.8 SEM analysis

The surface morphology of the hybrid salts  $[\text{DEDSA}]_3[\text{PMO}_{12}\text{O}_{40}]$  and  $[\text{DEDSA}]_3[\text{PW}_{12}\text{O}_{40}]$  were studied in SEM images at the same magnification in **Fig. 2.10**. The SEM topography reveals micrometer sized irregular agglomeration through extensive secondary interactions of intermolecular H-bonds of the two  $-\text{SO}_3\text{H}$  functionality of the ammonium cation with the oxygen atoms of Keggin anions. The exact reason for differences in the sizes of aggregates are unknown and it is beyond the scope of this study.



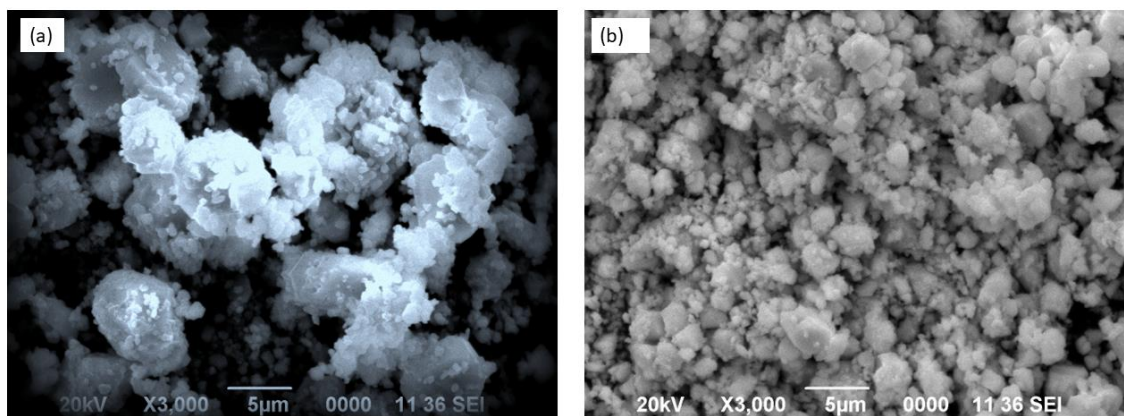


**Fig. 2.10:** SEM images of (a) [DEDSA]<sub>3</sub>[PMo<sub>12</sub>O<sub>40</sub>] and (b) [DEDSA]<sub>3</sub>[PW<sub>12</sub>O<sub>40</sub>].

### 2.2.9 EDX analysis

Energy Dispersive X-ray (EDX) spectrum of the [DEDSA]<sub>3</sub>[PMo<sub>12</sub>O<sub>40</sub>] in **Fig. 2.11a** confirmed C, N, O, P, Mo and S as the constituent elements of the hybrid compound, whereas the spectrum of [DEDSA]<sub>3</sub>[PW<sub>12</sub>O<sub>40</sub>] in **Fig. 2.11b** displayed all the peaks of constituent elements except phosphorus. It can be accounted for low abundance of this element in surface of the Keggin structured anion as compared to high abundances of W and O elements. At the same, the presence of P in the phosphotungstate Keggin anion can be confirmed from the <sup>31</sup>P NMR spectrum of [DEDSA]<sub>3</sub>[PW<sub>12</sub>O<sub>40</sub>], **Fig. 2.4b**.

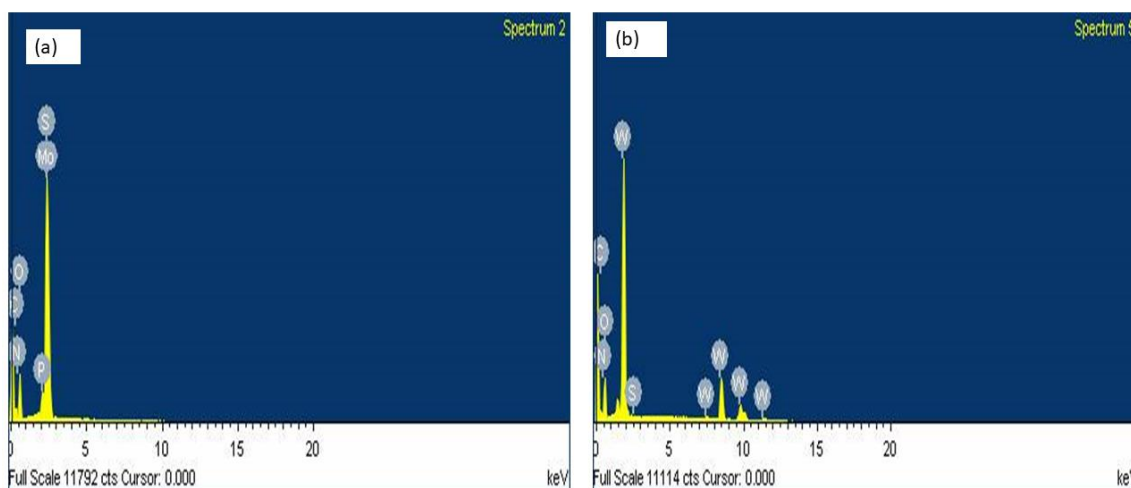
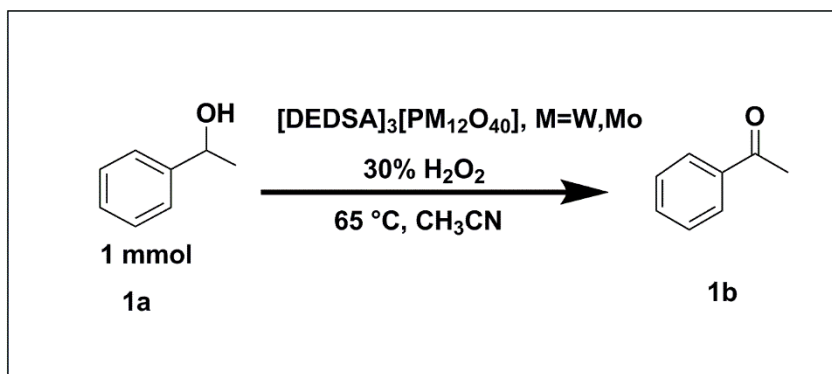


**Fig. 2.11:** EDX patterns of (a) [DEDSA]<sub>3</sub>[PMo<sub>12</sub>O<sub>40</sub>] and (b) [DEDSA]<sub>3</sub>[PW<sub>12</sub>O<sub>40</sub>].

## 2.3 Catalytic activity

### 2.3.1 Optimization of reaction condition



**Scheme 2.2:** Model reaction for oxidation of alcohol.

To study the redox properties of POM hybrid catalysts, initially we optimized the amount of  $[\text{DEDSA}]_3[\text{PW}_{12}\text{O}_{40}]$  by taking 0.5, 2 and 3 mol% of the catalyst for oxidation (**Scheme 2.2**) of 1-phenylethanol (1 mmol) in  $\text{CH}_3\text{CN}$  (2 mL) using 30%  $\text{H}_2\text{O}_2$  (3 mmol) at different temperature (0 °C, 25 °C, 45 °C, 65 °C, 82 °C) for the specified reaction time as included in **Table 2.2** (entries 1-7). Excellent catalytic activity was observed with 3 mol% of the  $[\text{DEDSA}]_3[\text{PW}_{12}\text{O}_{40}]$  at 65 °C for 2 hours to produce 98% yield of acetophenone (**Table 2.2**, entry 4). Using the same amount of  $[\text{DEDSA}]_3[\text{PMo}_{12}\text{O}_{40}]$  catalyst, the product yield was seen to decrease at 65 °C (**Table 2.2**, entry 8). It was also observed that trace amount of alcohol conversion occurred in absence of catalyst using 30%  $\text{H}_2\text{O}_2$  (3 mmol) at 65 °C in acetonitrile (**Table 2.2**, entry 9). So, 3 mol% of  $[\text{DEDSA}]_3[\text{PW}_{12}\text{O}_{40}]$  was taken as the standard amount to study the effect of solvents for the model reaction in **Table 2.3**. The redox properties of both of these POM hybrid catalysts were observed to be slightly different with respect to the catalyst amount which was better for the  $[\text{DEDSA}]_3[\text{PW}_{12}\text{O}_{40}]$  catalyst (**Table 2.2**, entry 4). This can be attributed for varied coordination abilities of Mo(VI) and W(VI) cations and also different metal-oxygen bond order in their respective *in situ* generated active species peroxophosphotungstate  $\{\text{PO}_4[\text{WO}(\text{O}_2)_2]_4\}^{3-}$  and peroxophosphomolybdate  $\{\text{PO}_4[\text{MoO}(\text{O}_2)_2]_4\}^{3-}$  as proposed in **Scheme 2.3** for catalytic oxidation of alcohol involving hydrogen peroxide as oxidant [55]. During the oxidation process, the reaction intermediate of alcohol with  $\{\text{PO}_4[\text{MoO}(\text{O}_2)_2]_4\}^{3-}$  will be more stable with refilling of electrons in three vacant orbitals 4f, 4d, and 5s of the Mo species as compared to the intermediate of  $\{\text{PO}_4[\text{WO}(\text{O}_2)_2]_4\}^{3-}$  involving two vacant orbitals, 5d and 6s of the W cation. When the temperature was increased from 65 °C to 82 °C, the oxidation of alcohol was completed within 1.5 hour with lowering of selectivity and yield of acetophenone

through formation of byproduct that can be attributed for formation of over oxidized product at 82 °C involving H<sub>2</sub>O<sub>2</sub> as oxidant (**Table 2.2**, entry 5).

**Table 2.2.** Study of temperature effects and catalyst amount for the model reaction

Entry	Reaction Temperature (°C)	Time(h)	Catalyst amount <sup>[a]</sup> (mol%)	Yield % <sup>[b]</sup>
1.	0	8	3	0
2.	25	8	3	0
3.	45	6	3	58
4.	65	2	3	98
5.	82	1.5	3	82
6.	65	2	0.5	16
7.	65	2	2	70
8.	65	2.5	3	88
9.	65	8	0	Trace amount

<sup>[a]</sup> Reaction conditions: (i) using [DEDSA]<sub>3</sub>[PW<sub>12</sub>O<sub>40</sub>] catalyst: 1-phenylethanol (1 mmol), 30% H<sub>2</sub>O<sub>2</sub> (3 mmol), CH<sub>3</sub>CN (2 mL) (entries 1-7); (ii) using [DEDSA]<sub>3</sub>[PMo<sub>12</sub>O<sub>40</sub>] catalyst (entries 8); (iii) without catalyst (entry 9); <sup>[b]</sup> Yield % of acetophenone based on GC analysis

### 2.3.2 Effect of solvent study

Solvent study was conducted by performing the oxidation of 1-phenylethanol in polar solvent including H<sub>2</sub>O, MeOH, CH<sub>3</sub>CN, EtOAc at 65 °C and in non-polar solvent like CH<sub>2</sub>Cl<sub>2</sub>, hexane in reflux temperature with the optimized amount of [DEDSA]<sub>3</sub>[PW<sub>12</sub>O<sub>40</sub>] catalyst for 2-8 hours (**Table 2.3**). The results in **Table 2.3** expressed solvent dependence catalytic activity of the POM hybrid with varied yields of oxidized product which were observed to proceed through either homogeneous or heterogeneous catalytic phases in reaction media. The catalyst was seen to be soluble in MeOH, CH<sub>3</sub>CN as polar solvents (**Table 2.3**, entries 2, 3) except water making the reaction as homogeneous catalysis and the percentage yield of products were raised to higher levels. At the same time, the insolubility of catalyst in H<sub>2</sub>O, CH<sub>2</sub>Cl<sub>2</sub> and n-hexane converts the reaction as heterogeneous catalysis and pulling down the percentage yields (**Table 2.3**, entries 1, 4, 5). In case of ethyl acetate solvent, the catalyst was found to form an separate phase in the reaction medium making the reaction system non homogeneous in nature that may be accounted for moderate yield of the product (**Table 2.3**, entry 7). The self-precipitation of the [DEDSA]<sub>3</sub>[PW<sub>12</sub>O<sub>40</sub>] catalyst from the reaction mixture was done by pouring CH<sub>2</sub>Cl<sub>2</sub> solvent in the crude product mixture of oxidation obtained **Fig. 2.12a** after evaporation of the homogeneous solution of reaction in acetonitrile under reduced pressure. The catalyst

was recovered and reused after filtration of the dichloromethane solution containing oxidation product by keeping in vacuum oven for 5 hours at 80 °C. The other polyoxometalate catalyst [DEDSA]<sub>3</sub>[PMO<sub>12</sub>O<sub>40</sub>] also displayed similar solubility behavior with these solvents which was represented in **Fig. 2.12b** for the model reaction in acetonitrile. The solvent dependent behavior of the organic-inorganic IL-POM based hybrids towards polar and non-polar solvent can be considered as a combined outcome of secondary interactions including H-bonding, ion-dipole interactions etc. for each ionic component of the POM with the solvent molecules. The inability of water to solubilize the catalyst can be expected for insufficient H-bonding interaction with the water molecules in presence of two hydrophobic ethyl groups tethered to the ammonium cation of hybrid salt. This factor may become a preferential condition for self-aggregation of the POM hybrid in water through intermolecular H-bonding interactions involving the POM anion and -SO<sub>3</sub>H groups of the ammonium cation of the hybrid material. The non-polar solvents like dichloromethane, hexane etc. are favorable for self-aggregation of the POM hybrids. In MeOH and CH<sub>3</sub>CN,

each of the ionic component of POM hybrid can make sufficient intermolecular H-bonding as well as ion-dipole interactions with the solvent molecules in presence of slight amount of miscible water which may increase the solubility of the catalyst.

**Table 2.3.** Study of solvent effects for the model reaction using [DEDSA]<sub>3</sub>[PW<sub>12</sub>O<sub>40</sub>] catalyst

Entry	Solvent	Time (h)	Temperature <sup>[a]</sup> °C	Yield% <sup>[a,b]</sup>
1.	H <sub>2</sub> O	8	65	45
2.	CH <sub>3</sub> OH	5	65	78
3.	CH <sub>3</sub> CN	2	65	98
4.	CH <sub>2</sub> Cl <sub>2</sub>	8	39	10
5.	n-Hexane	8	68	>10
6.	Solvent-free	3	65	60
7.	Ethyl acetate	3	65	66

<sup>[a]</sup>Reaction conditions: 1-phenylethanol (1mmol), 30% H<sub>2</sub>O<sub>2</sub> (3 mmol), [DEDSA]<sub>3</sub>PW<sub>12</sub>O<sub>40</sub> (3 mol%) catalyst, CH<sub>3</sub>CN (2 mL).

<sup>[b]</sup>Yield % based on starting substrates in GC analysis

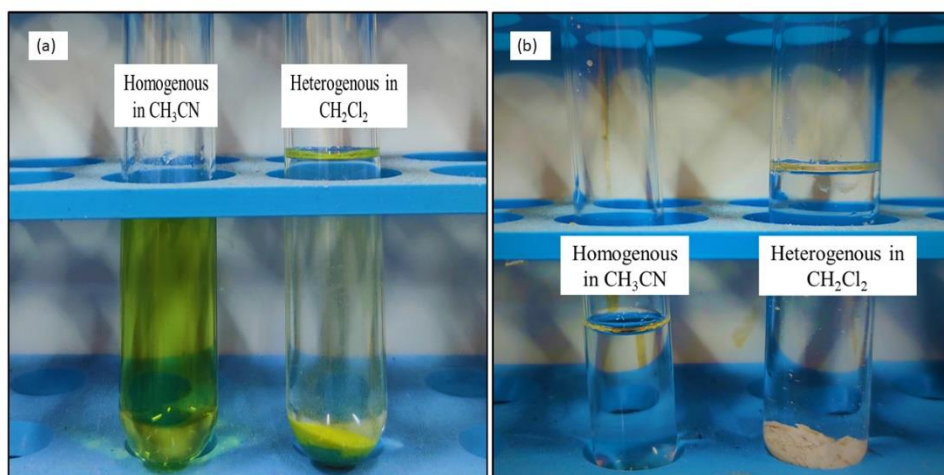


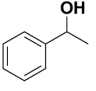
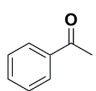
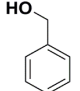
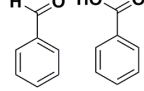
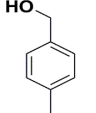
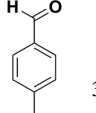
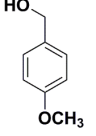
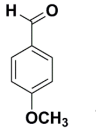
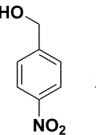
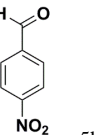
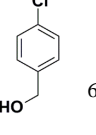
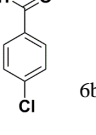
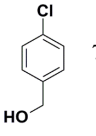
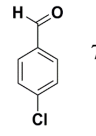
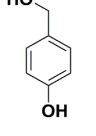
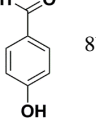
**Fig. 2.12:** Photographs of (a)  $[\text{DEDSA}]_3[\text{PMO}_{12}\text{O}_{40}]$  and (b)  $[\text{DEDSA}]_3[\text{PW}_{12}\text{O}_{40}]$  switching from homogeneous reaction medium in left testtube to heterogeneous one by self-precipitating in testtube kept in right after evaporation of acetonitrile solvent and pouring dry  $\text{CH}_2\text{Cl}_2$  afterwards.

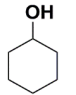
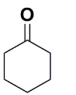
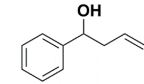
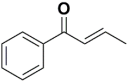
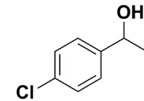
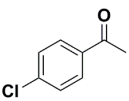
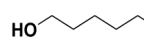
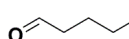
### 2.3.3 Substrate scope study

The substrate scope study of oxidation reaction was investigated in acetonitrile solution for different substituted benzyl alcohol or cyclic/acyclic secondary alcohol under the optimized condition using  $[\text{DEDSA}]_3[\text{PW}_{12}\text{O}_{40}]$  as catalyst (**Table 2.4**). The rate of oxidation was found to be relatively high with 3 mol% of the catalyst in case of *p*-methoxy benzyl alcohol and *p*-hydroxy benzyl alcohol (**Table 2.4**, entries 4,8) because of strong mesomeric effect as compared to *p*-chloro benzyl alcohol (**Table 2.4**, entry 6). The electron donating substituents in benzyl alcohol expressed excellent yields (**Table 2.4**, entry 3) while the substrates with electron withdrawing group showed relatively low reactivity (**Table 2.4**, entries 5, 6) as observed from GC analysis. The % yield of oxidised product of *p*-chloro benzyl alcohol increased slightly after increasing the catalyst amount up to 4 mol% (**Table 2.4**, entry 7) within 6.5 h reaction at 65 °C in  $\text{CH}_3\text{CN}$ . Surprisingly, the optimized amount of catalyst did not work with cyclohexanol and even after increasing the catalyst amount upto 4 mol % (**Table 2.4**, entry 9) at the temperature of 65 °C. Acyclic 2° alcohols like 1-phenylethanol and *p*-chloro-1 phenylethanol proceeded efficiently for 2-3 hours reaction with varied amount of the catalyst (**Table 2.4**, entries 1, 11). In case of oxidation of 4-phenyl-1-buten-4-ol, a rearranged  $\alpha, \beta$  unsaturated keto compound was formed after shifting of double bond position without oxidation (**Table**

2.4, entry 10). No carbonyl products were obtained under the optimized condition for oxidation of primary alcohol other than benzylic alcohol (Table 2.4, entry 12).

**Table 2.4.** Substrate scope for oxidation of alcohols using organic-inorganic IL-POM based hybrid

Entry	Substrate	Product	Time(h)	Yield (%) <sup>[c]</sup>
1. <sup>[a]</sup>	 1a	 1b	2	98
2. <sup>[a]</sup>	 2a	 2b 2c	6	88 (2b) 9 (2c)
3. <sup>[a]</sup>	 3a	 3b	2	93
4. <sup>[a]</sup>	 4a	 4b	1	98
5. <sup>[a]</sup>	 5a	 5b	6	79
6. <sup>[a]</sup>	 6a	 6b	6.5	55
7. <sup>[b]</sup>	 7a	 7b	6.5	60
8. <sup>[a]</sup>	 8a	 8b	1	93

9. <sup>[b]</sup>	 9a	 9b	6	0
10. <sup>[a]</sup>	 10a	 10b	3	68
11. <sup>[b]</sup>	 11a	 11b	3	77
12. <sup>[a]</sup>	 12a	 12b	6	0

<sup>[a]</sup> Reaction conditions: alcohol (1 mmol), H<sub>2</sub>O<sub>2</sub> (3 mmol), [DEDSA]<sub>3</sub>PW<sub>12</sub>O<sub>40</sub> (3 mol%), CH<sub>3</sub>CN (2 mL), 65 °C.

<sup>[b]</sup> Reaction conditions: alcohol (1 mmol), H<sub>2</sub>O<sub>2</sub> (3 mmol), [DEDSA]<sub>3</sub>PW<sub>12</sub>O<sub>40</sub> (4 mol%), CH<sub>3</sub>CN (2 mL), 65 °C.

<sup>[c]</sup> GC yields based on starting substrates

## 2.4 Plausible reaction mechanism

The mechanism (**Scheme 2.3**) demonstrates that the Keggin polyanion in the organic-inorganic IL-POM based hybrids gets degraded in presence of H<sub>2</sub>O<sub>2</sub> to an active metal peroxo intermediate {PO<sub>4</sub>[MO(O<sub>2</sub>)<sub>2</sub>]<sub>4</sub>}<sup>3-</sup>, which is found to be responsible for the oxidation reaction [7, 56, 57]. This was further evidenced from respective IR spectrum of peroxo intermediate isolated after treatment of the [DEDSA]<sub>3</sub>PW<sub>12</sub>O<sub>40</sub> with H<sub>2</sub>O<sub>2</sub> solution at room temperature (**Fig. 2.13**). The spectrum displayed peaks at 857 cm<sup>-1</sup> for ν(O-O) vibration, 555 cm<sup>-1</sup> for symmetric metal–oxygen (W–O<sub>2</sub>) stretching frequency and 677 cm<sup>-1</sup> for asymmetric (W–O<sub>2</sub>) stretching frequency which also proved the involvement of peroxophosphometalate intermediate in the oxidation reaction [58,59].

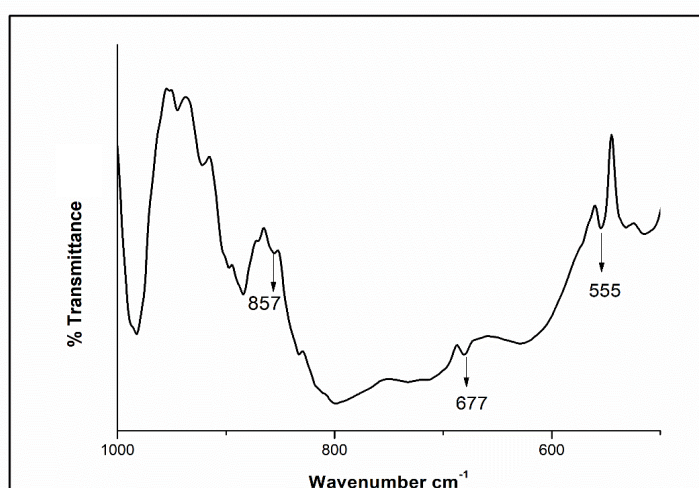
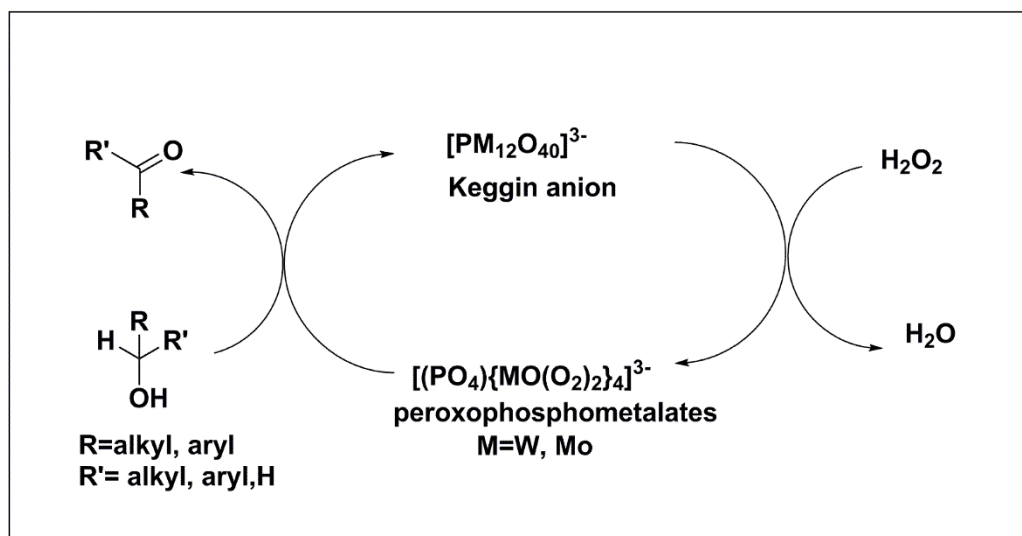


**Fig. 2.13:** FT-IR spectrum providing evidence of formation of peroxophosphometalates after treating [DEDSA]<sub>3</sub>PW<sub>12</sub>O<sub>40</sub> with H<sub>2</sub>O<sub>2</sub>.



**Scheme 2.3:** Mechanism of oxidation of alcohol using  $[DEDSA]_3PM_{12}O_{40}$  via peroxo intermediate formation.

## 2.5 Recyclability study of the catalyst

The catalytic recyclability was studied by taking 3 mmol of 1-phenylethanol as model substrate with the optimized amount of  $[DEDSA]_3PW_{12}O_{40}$  catalyst in  $CH_3CN$  at  $65\text{ }^\circ\text{C}$ . The catalyst was precipitated out from the homogeneous solution of acetonitrile through addition of dry  $CH_2Cl_2$  which is insoluble in  $CH_2Cl_2$ . The POM

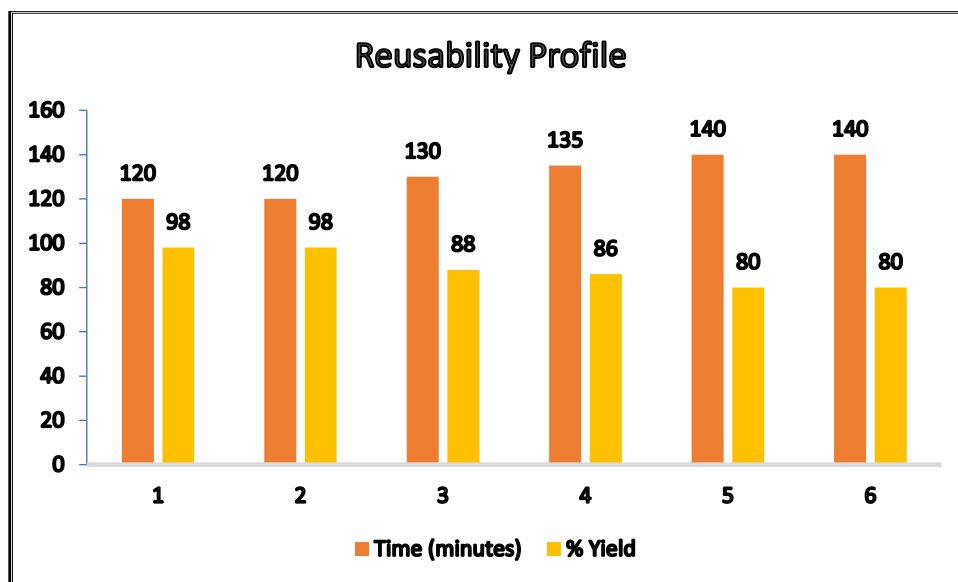


**Fig. 2.14:** Recyclability diagram of the  $[DEDSA]_3[PW_{12}O_{40}]$  for the model reaction.

catalyst was then washed with hexane and then reactivated in vacuum oven at  $80\text{ }^\circ\text{C}$  for 5 h for next catalytic run. **Fig. 2.14** displays reusability profile of the spent catalyst for seven



consecutive cycles. Similar catalytic activity with each cycle was observed till third run with modest decrease in yield after the fourth run. The reused catalyst almost retains the similar peaks of FT-IR spectrum compared to the fresh catalyst (**Fig. 2.15**) after the 7<sup>th</sup> cycle.

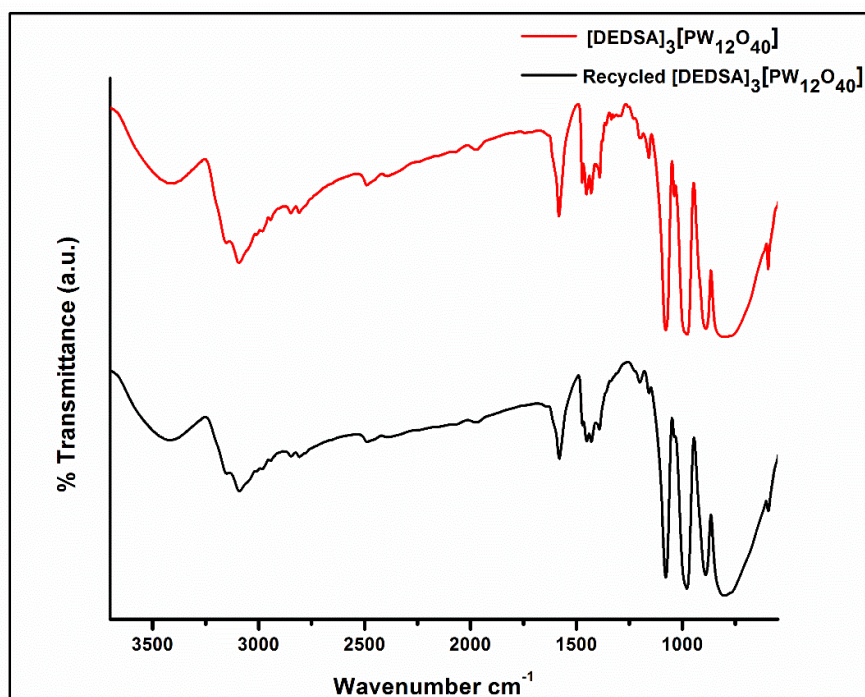


**Fig. 2.15:** FT-IR spectra of the fresh [DEDSA]<sub>3</sub>[PW<sub>12</sub>O<sub>40</sub>] and recycled [DEDSA]<sub>3</sub>[PW<sub>12</sub>O<sub>40</sub>] after 7<sup>th</sup> cycle.

## 2.6 Conclusions

Here in this work we designed and presented two novel solvent-responsive thermally stable -SO<sub>3</sub>H functionalized ammonium based polyoxometalate hybrids of phosphomolybdic acid and phosphotungstic acid as solid oxidation catalyst. Due to the presence of -SO<sub>3</sub>H group in the cation and its nature of hydrogen bonding with the solvent molecules as well with the anions led to the construction of a solvent responsive catalyst which proved as a great advantage while separating catalyst from the reaction medium. And also this property helped in switching between homogeneous and heterogeneous reaction systems. It was used as an efficient catalyst for selective oxidation of substituted benzylic alcohol to aldehydes and acyclic secondary alcohol to keto compounds using

hydrogen peroxide as a green oxidant. The catalyst was inactive for oxidation of cyclic secondary alcohol. It also acted as chemoselective oxidant for oxidation of secondary alcohol containing double bond to keto compound with rearrangement of the double bond in  $\alpha$ ,  $\beta$  position with respect to the carbonyl group. Because of the high thermal stability, high catalytic activity and ease in recovery and reuse enhances this method to be an environment friendly and simpler way for oxidation of alcohols to aldehydes and ketones. Thus we were able to design functionalized organic-inorganic IL-POM based hybrids which acted as solvent-responsive self-separation catalyst. Introduction of sulfonic groups and hydrophobic groups like ethyl in the cationic counterpart and their interaction with the anion as well as solvent molecules resulted in solvent responsive nature in the hybrids.

## 2.7 Experimental section

### 2.7.1 Procedure of synthesis of diethyldisulfoammonium salts of Keggin anions [DEDSA]<sub>3</sub>[PM<sub>12</sub>O<sub>40</sub>] where M= Mo (VI), W(VI)

The -SO<sub>3</sub>H functionalized POM hybrid salt [DEDSA]<sub>3</sub>[PM<sub>12</sub>O<sub>40</sub>] where M= Mo (VI), W(VI) of diethyldisulfoammonium cation containing polyoxometalate Keggin anion [PMo<sub>12</sub>O<sub>40</sub>]<sup>3-</sup> or [PW<sub>12</sub>O<sub>40</sub>]<sup>3-</sup> were prepared in two steps (**Scheme 2.1**). Firstly, the initial ionic liquid diethyl disulfoammonium chloride ([DEDSA]Cl) was prepared by dropwise addition of chlorosulfonic acid (30 mmol) using dropping funnel into a stirring solution of diethylamine (15 mmol) in dry CH<sub>2</sub>Cl<sub>2</sub> (15 mL) in a two neck 100 mL round bottom flask at 0 °C for 10 minutes with continuous stirring [60]. Then it was stirred for one hour at room temperature to get a separate layer of the [DEDSA]Cl in dichloromethane solvent. Repeated washing of the reaction mixture with dry CH<sub>2</sub>Cl<sub>2</sub> (3 × 10 mL) and followed by decantation remove most of the soluble impurities in dichloromethane. The crude [DEDSA]Cl was obtained as pure light red yellowish liquid after drying in vacuum oven at 50 °C. The formation of this ionic liquid was confirmed from <sup>1</sup>H NMR and <sup>13</sup>C NMR. The <sup>1</sup>H NMR and <sup>13</sup>C NMR spectra of [DEDSA]Cl is provided below in the section containing spectral data regarding all synthesized compounds.

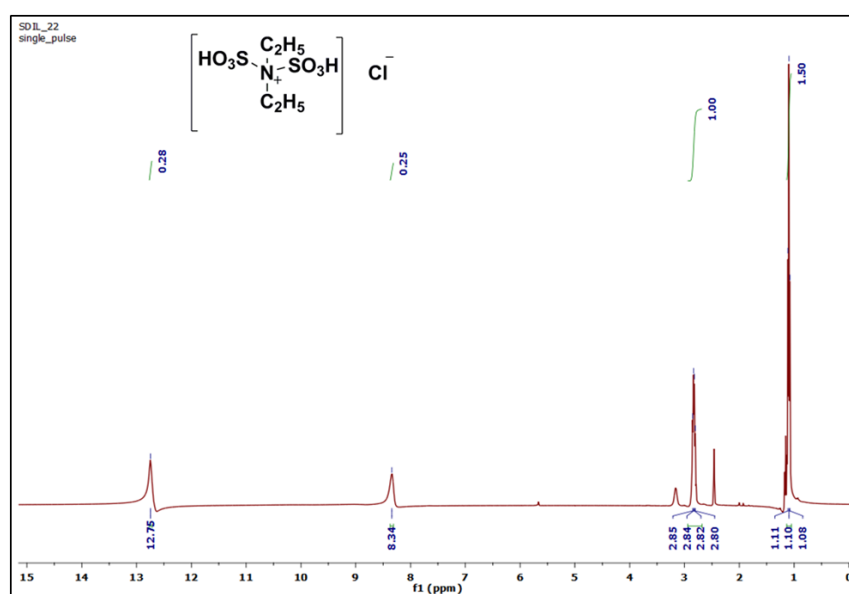
In second step, 1 mmol of the heteropolyacid (HPA), H<sub>3</sub>PMo<sub>12</sub>O<sub>40</sub>·nH<sub>2</sub>O (PMA) or H<sub>3</sub>PW<sub>12</sub>O<sub>40</sub>·nH<sub>2</sub>O (PTA) (**Fig. 2.6**) was dissolved in 20 mL of distilled water at room temperature in a 100 mL round bottom flask by continuous stirring. To the stirred solution of HPA, 3 mmol of [DEDSA]Cl·nH<sub>2</sub>O (**Fig. 2.6**) was added dropwise within 5 minutes. Immediately yellow and white precipitation were observed for [DEDSA]<sub>3</sub>[PMo<sub>12</sub>O<sub>40</sub>] and

[DEDSA]<sub>3</sub>[PW<sub>12</sub>O<sub>40</sub>] respectively. The reaction was continued to stir for another 12 hours to complete the precipitation of organic-inorganic IL-POM based hybrids in water. The product mixture was centrifuged to obtain the organic-inorganic IL-POM based hybrids i.e. [DEDSA]<sub>3</sub>[PW<sub>12</sub>O<sub>40</sub>] and [DEDSA]<sub>3</sub>[PMo<sub>12</sub>O<sub>40</sub>] as water insoluble solids which were washed 3-4 times with distilled water to get analytically pure product. Then the isolated solid products were dried in vacuum oven at 80 °C for 12 hours to get 97-99% yields.

### 2.7.2 General procedure for oxidation of alcohols

In a typical experiment, a homogeneous solution of 1 mmol of 1-phenylethanol and 3 mol% of [DEDSA]<sub>3</sub>[PW<sub>12</sub>O<sub>40</sub>] catalyst in CH<sub>3</sub>CN (2 mL) was stirred at 65 °C using 30% H<sub>2</sub>O<sub>2</sub> (3 mmol) as oxidant for 2 hours in a 100 mL two necked round bottom flask fitted with an air condenser in an oil bath. After completion of the reaction as monitored from thin layer chromatographic technique, the acetonitrile solvent was evaporated under reduced pressure and CH<sub>2</sub>Cl<sub>2</sub> was poured over the remaining product mixture. Catalyst self-precipitates in CH<sub>2</sub>Cl<sub>2</sub> and product being soluble in the CH<sub>2</sub>Cl<sub>2</sub> was separated by simple filtration. The catalyst was washed with more amount of the CH<sub>2</sub>Cl<sub>2</sub> solvent (2 × 2 mL) followed by distilled water. The spent catalyst was reactivated after drying in vacuum oven at 80 °C for 5 hours to make ready for next cycle of the oxidation reaction.

### 2.8 NMR spectra of [DEDSA]Cl



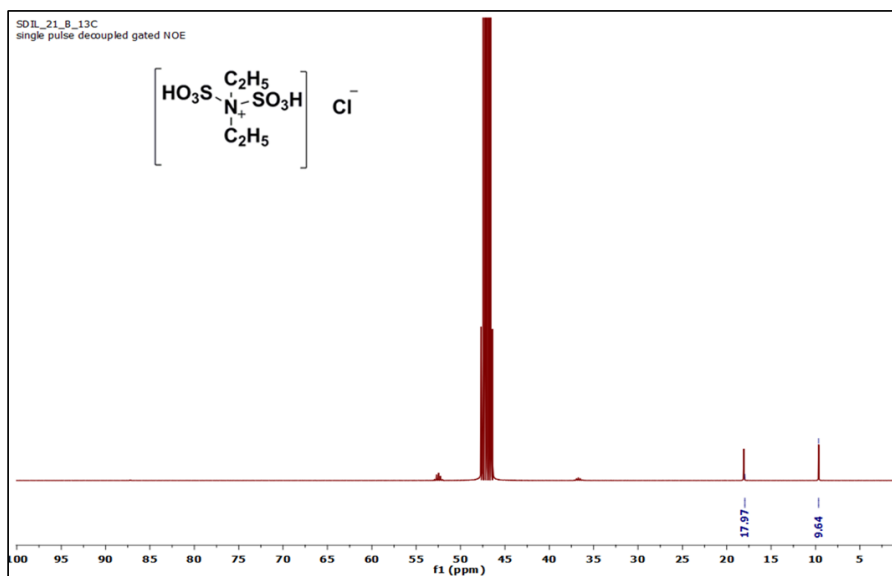


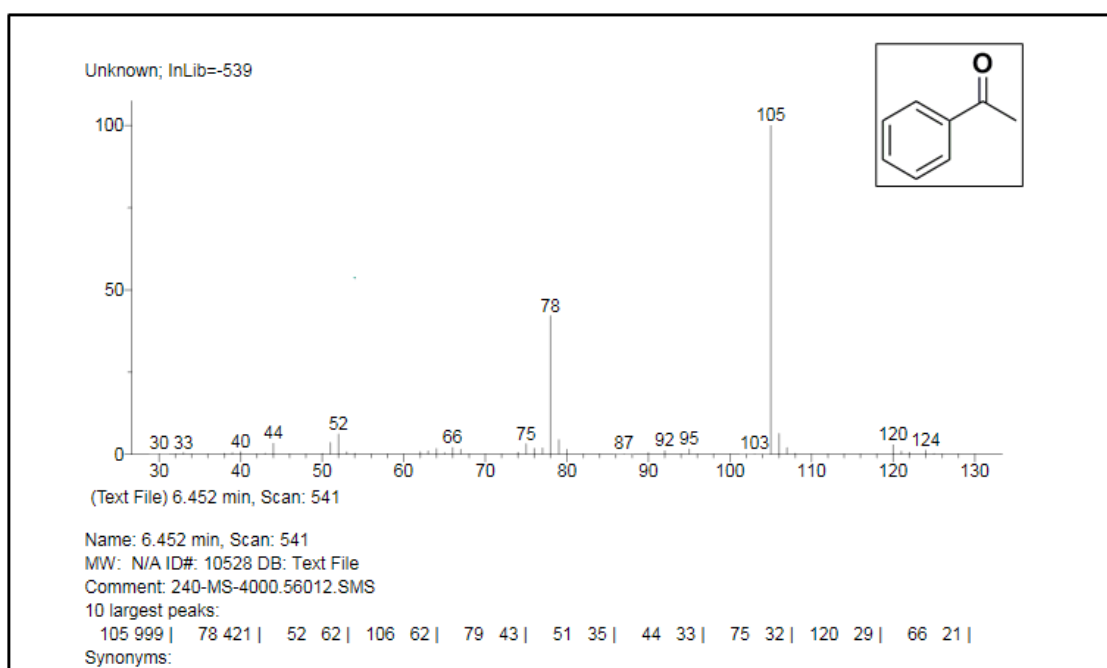
**Fig. 2.16:** (a)  $^1\text{H}$  NMR spectrum of [DEDSA]Cl and (b)  $^{13}\text{C}$  NMR spectrum of [DEDSA]Cl.

**Table 2.5.** Spectral data of the parent ionic liquid and ionic liquid-polyoxometalate hybrids

Structure	Spectral data
$\left[ \text{HO}_3\text{S}-\text{N}^+(\text{C}_2\text{H}_5)_2-\text{SO}_3\text{H} \right] \text{Cl}^-$ [DEDSA]Cl	Light red yellowish liquid; FT-IR(KBr) $\nu \text{ cm}^{-1} = 3409, 2927, 2864, 1630, 1451, 1388, 1149, 1048, 869, 566$ ; $^1\text{H}$ NMR (DMSO- $d_6$ , 400MHz): $\delta$ 1.10 (t, $J=8.0$ Hz, 6H), 2.83 (q, $J=8$ Hz, 4H), 8.34 (s, 1H), 12.75 (s, 1H); $^{13}\text{C}$ NMR ( DMSO- $d_6$ , 100MHz) : $\delta$ 17.9, 9.6 ; CHN analysis : Calculated for [DEDSA]Cl (%): C 17.81, N 5.19, H 4.48 Found: C 17.72, N 5.29, H 4.52.
$\left[ \text{HO}_3\text{S}-\text{N}^+(\text{C}_2\text{H}_5)_2-\text{SO}_3\text{H} \right]_3 \text{PMo}_{12}\text{O}_{40}^{3-}$ [DEDSA] $_3$ [PMo $_{12}$ O $_{40}$ ]	Yellow solid; FT-IR(KBr) $\nu \text{ cm}^{-1} = 3433, 3152, 3109, 2943, 2844, 1583, 1452, 1391, 1204, 1151, 1065, 956, 870, 792, 593$ ; $^1\text{H}$ NMR (DMSO- $d_6$ , 400MHz): $\delta$ 1.12 (t, $J=8.0$ Hz, 6H), 2.87 (q, $J=8.0$ Hz, 4H), 8.15 (s, 2H); $^{13}\text{C}$ NMR (DMSO- $d_6$ , 100MHz): $\delta$ 41.83, 11.63; $^{31}\text{P}$ NMR (DMSO- $d_6$ , 202 MHz): $\delta$ -3.65. CHN

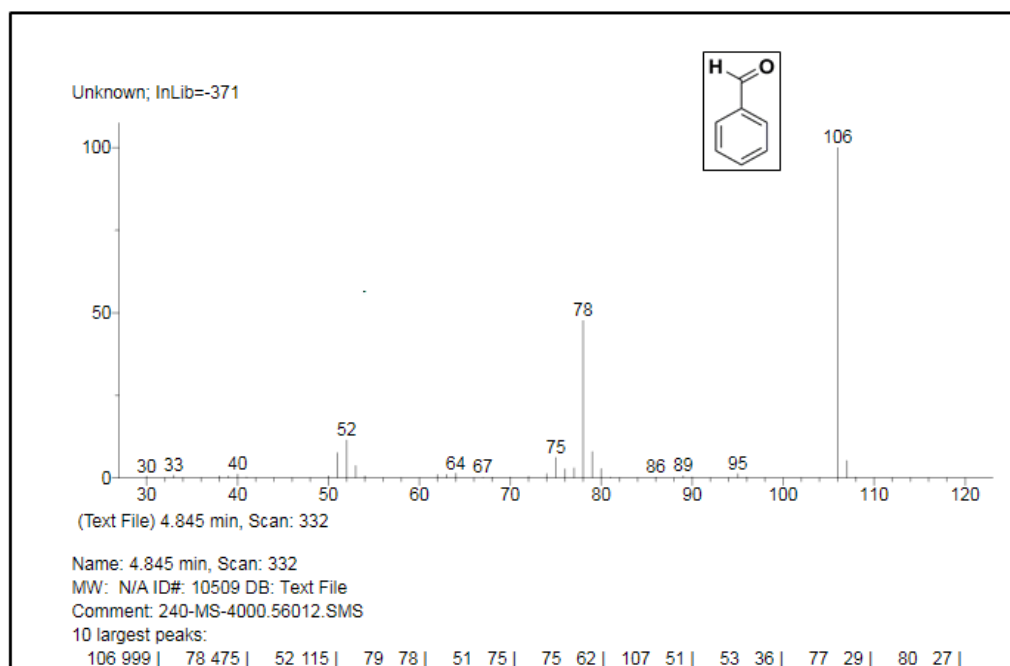
	analysis: Calculated for [DEDSA] <sub>3</sub> [PMo <sub>12</sub> O <sub>40</sub> ] (%): C 5.70, N 1.66, H 1.44 Found: C 5.88, N 1.72, H 1.37.  Melting point > 250 °C
$\left[ \begin{array}{c} \text{HO}_3\text{S} \\   \\ \text{N}^+ \\   \\ \text{C}_2\text{H}_5 \\   \\ \text{SO}_3\text{H} \\   \\ \text{C}_2\text{H}_5 \end{array} \right]_3 \text{PW}_{12}\text{O}_{40}^{3-}$ [DEDSA] <sub>3</sub> [PW <sub>12</sub> O <sub>40</sub> ]	White solid; FT-IR(KBr) $\nu$ cm <sup>-1</sup> =3433, 3152, 3091, 2943, 2844, 1583, 1452, 1391, 1193, 1151, 1065, 977, 888, 792, 593; <sup>1</sup> HNMR (DMSO- <i>d</i> <sub>6</sub> , 400MHz): $\delta$ 1.12 (t, <i>J</i> = 8.0 Hz, 6H), 2.88 (q, <i>J</i> = 8.0 Hz, 4H), 8.14 (s, 2H) ; <sup>13</sup> CNMR (DMSO- <i>d</i> <sub>6</sub> , 100MHz): $\delta$ 42.0, 11.63; <sup>31</sup> P NMR (DMSO- <i>d</i> <sub>6</sub> , 202 MHz): $\delta$ -15.15; CHN analysis: Calculated for [DEDSA] <sub>3</sub> [PW <sub>12</sub> O <sub>40</sub> ] (%): C 4.02, N 1.17, H 1.01. Found: C 4.15, N 1.22, H 1.11.  Melting point > 250 °C

## 2.9 Mass Spectra of products:



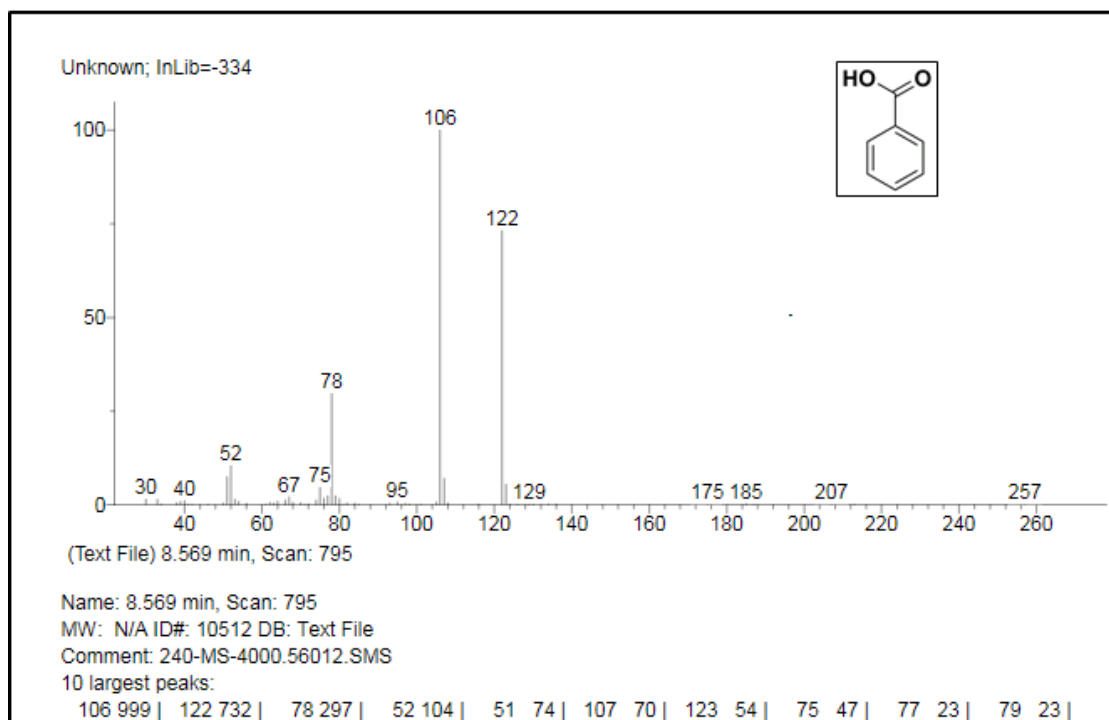
$m/z=120$  ( $M^+$ ), 105 (100 %), 78, 44

Mass spectra of **1b**



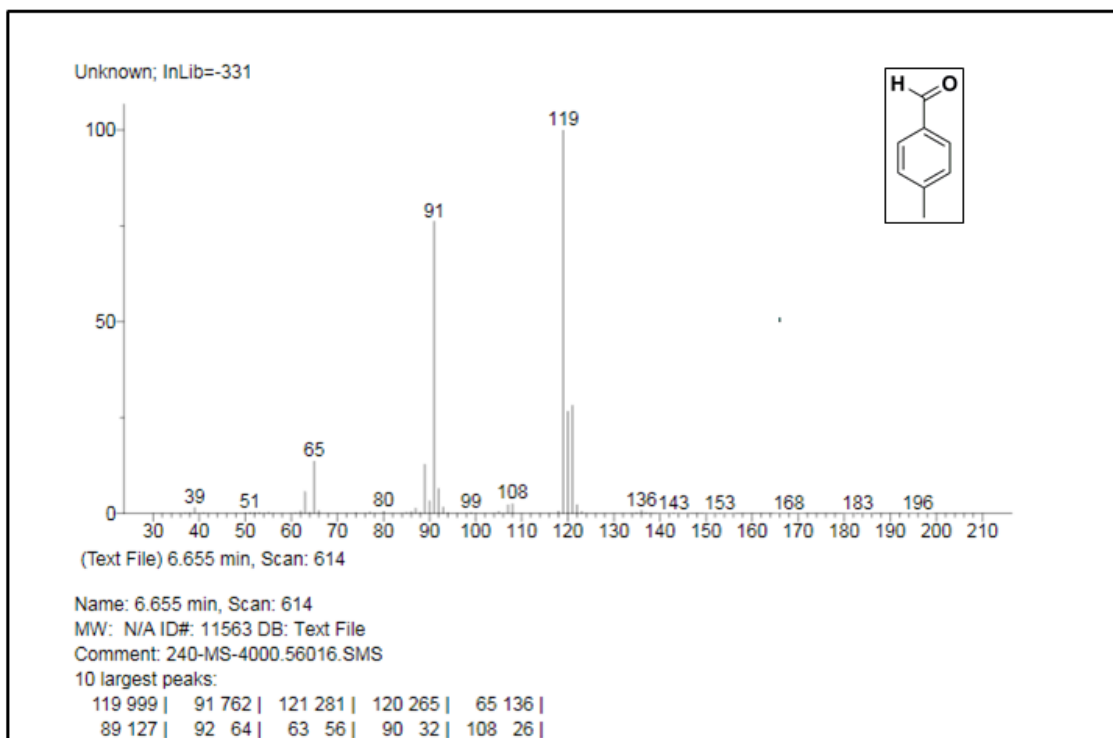
$m/z=106$  ( $M^+$ , 100 %), 78, 52

### Mass spectra of **2b**



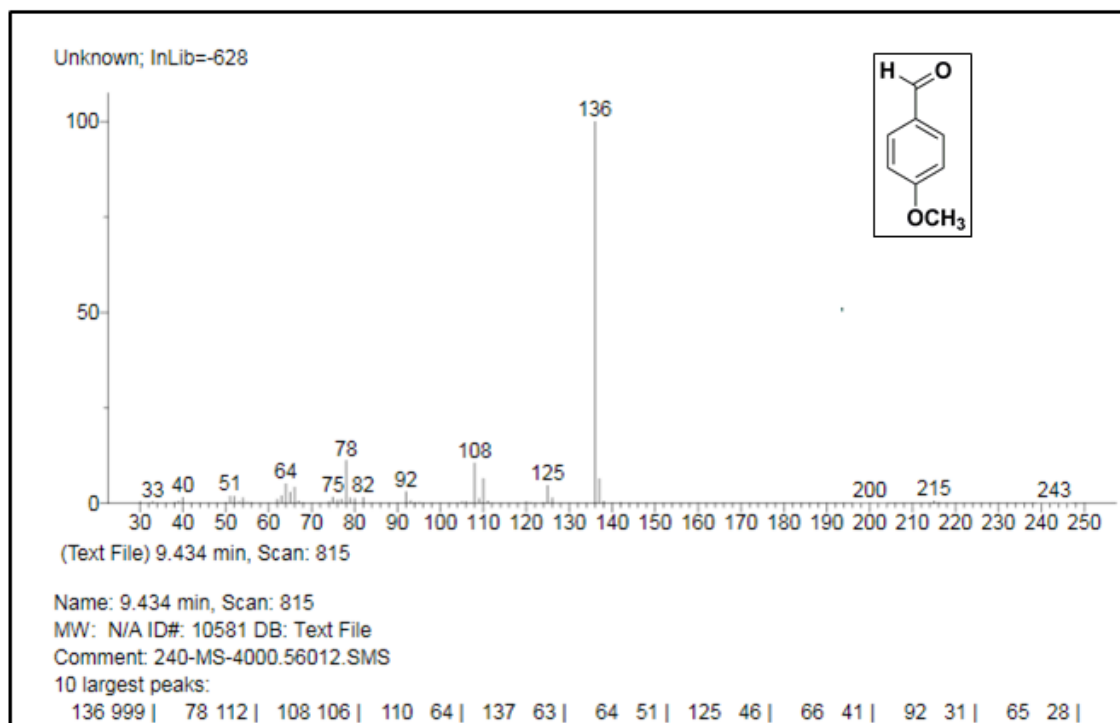
$m/z= (122 M^+), 106$  (100 %), 78, 52

### Mass spectra of **2c**



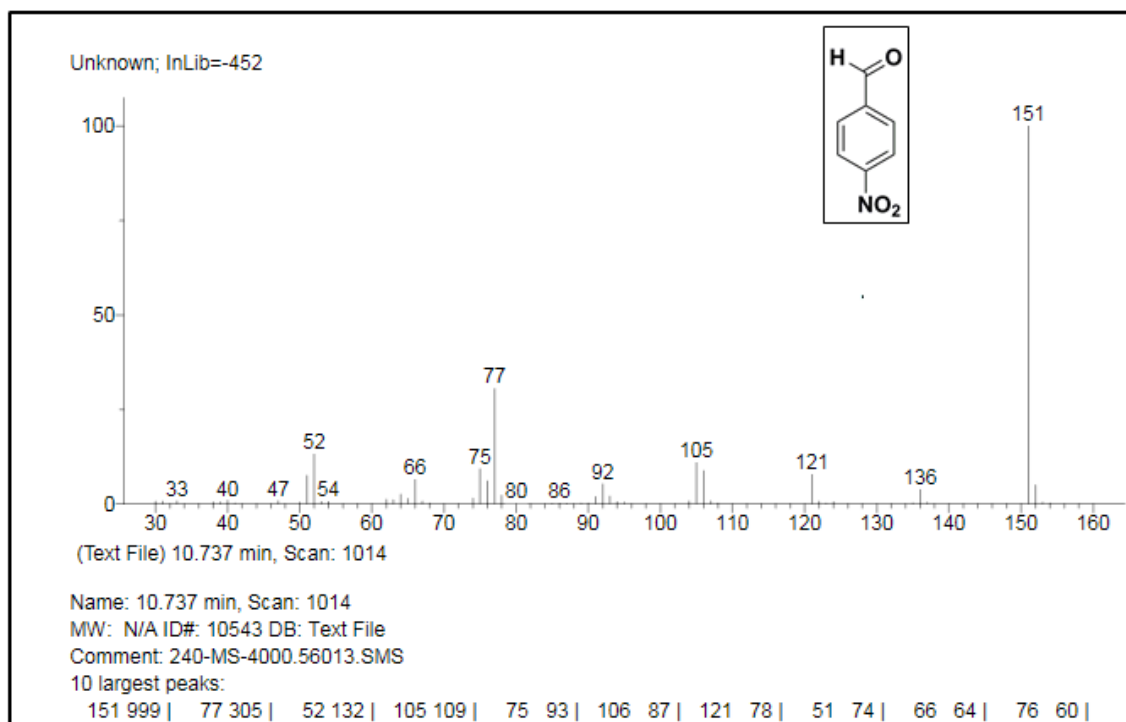
$m/z=120 (M^+)$ , 119 (100 %), 91

Mass spectra of **3b**



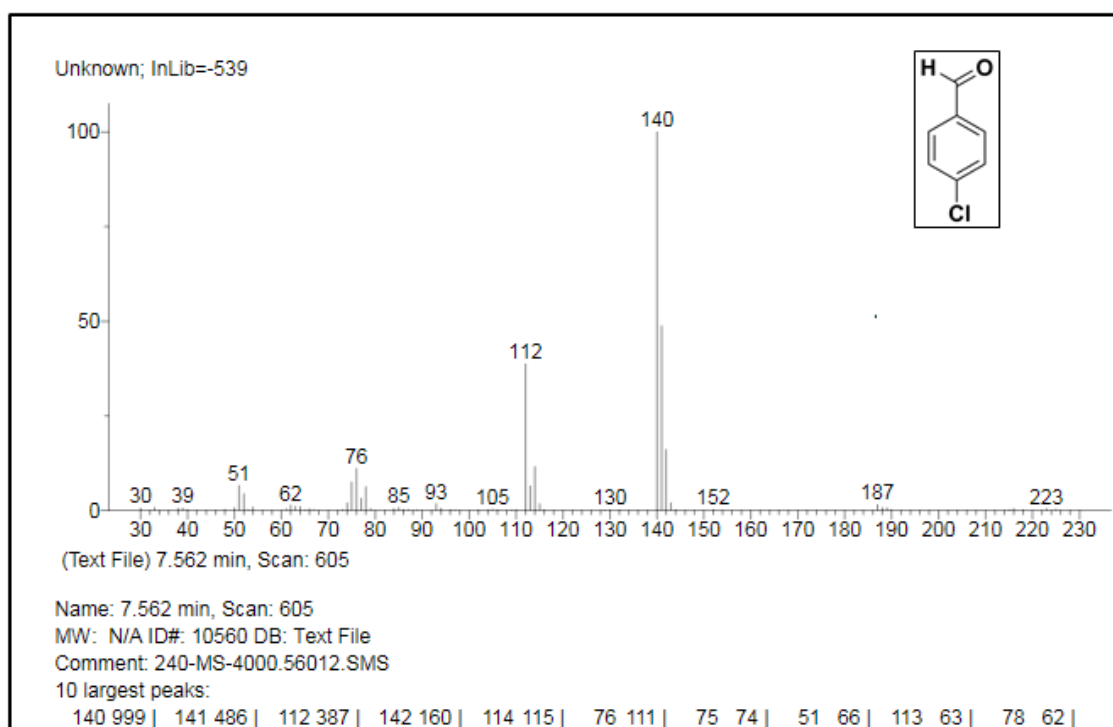
$m/z=136 (M^+)$ , 108, 78, 51

Mass spectra of **4b**



$m/z=151$  ( $M^+$ , 100%), 121, 105, 77, 75

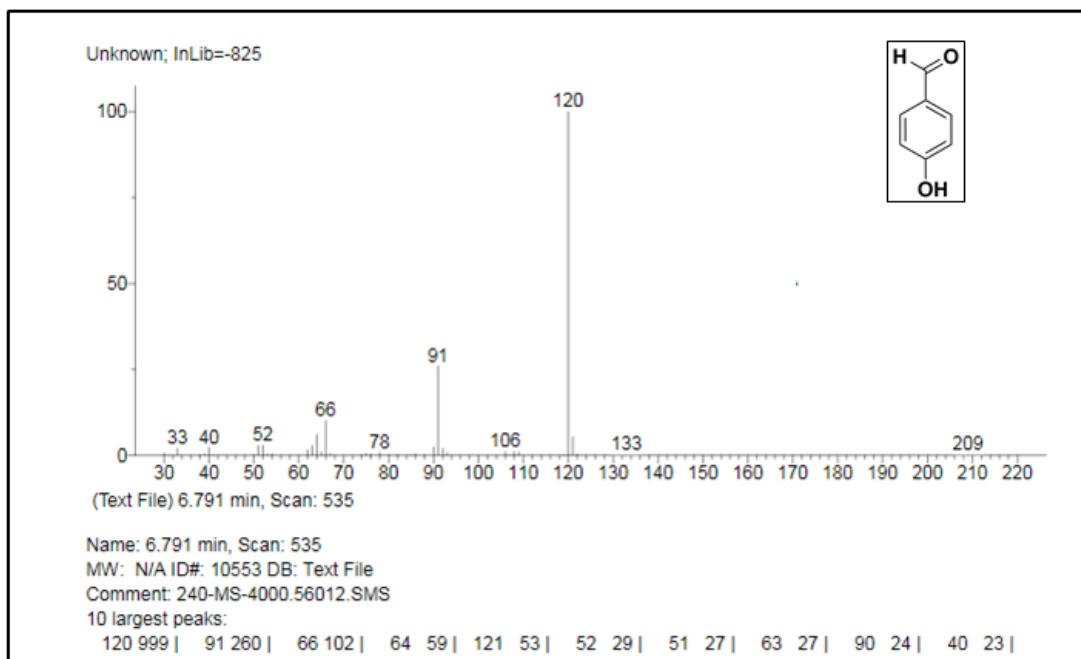
#### Mass spectra of **5b**



$m/z=140$  ( $M^+$ , 100 %), 112, 76, 52

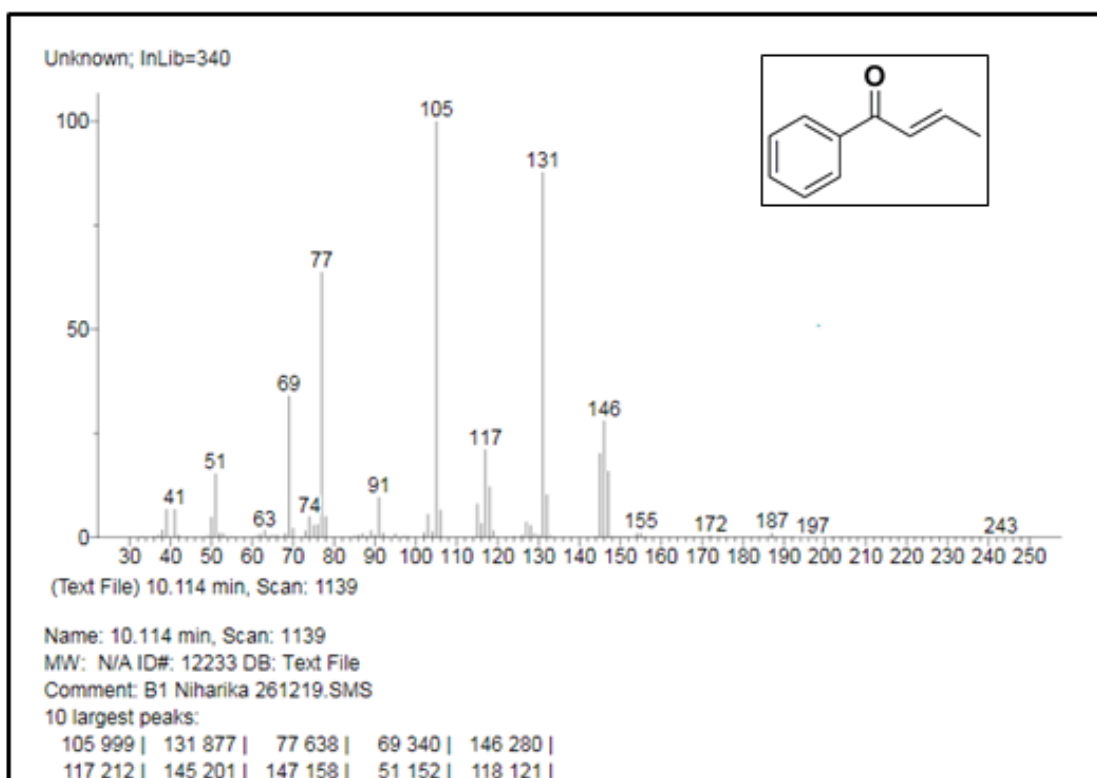
#### Mass spectra of **6b**





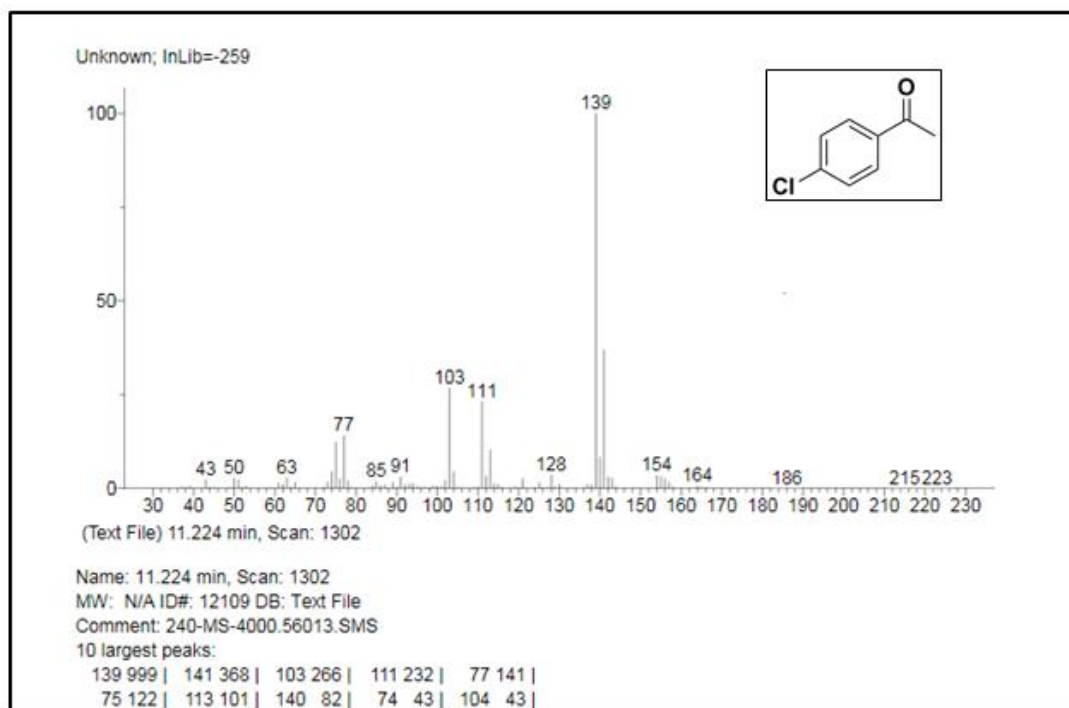
$m/z = 120$  (100 %), 106, 91, 78, 52

### Mass spectra of **8b**



$m/z = 146$  ( $M^+$ ), 131, 105 (100%), 91, 77, 69, 51

### Mass spectra of **10b**



$m/z = 154 (M^+), 139 (100\%), 111, 77, 43$

Mass spectra of **11b**

## 2.10 Bibliography

- [1] Ley, S. V., Norman, J., Griffith, W. P., and Marsden, S. P. Tetrapropylammonium perruthenate,  $Pr_4N^+ RuO_4^-$ , TPAP: A catalytic oxidant for organic synthesis. *Synthesis*, 1994(07): 639-666, 1994.
- [2] Ciriminna, R., Ghahremani, M., Karimi, B., and Pagliaro, M. Electrochemical alcohol oxidation mediated by TEMPO-like nitroxyl radicals. *ChemistryOpen*, 6(1): 5-10, 2017.
- [3] Sheldon, R. A., Arends, I. W., and Dijkstra, A. New developments in catalytic alcohol oxidations for fine chemicals synthesis. *Catalysis Today*, 57(1-2): 157-166, 2000.
- [4] Djerassi, C., Engle, R. R., and Bowers, A. The direct conversion of steroidal  $\Delta^5$ -3 $\beta$ -alcohols to  $\Delta^5$ - and  $\Delta^4$ -3-ketones. *Journal of Organic Chemistry*, 21(12): 1547-1549, 1956.
- [5] Cainelli, G. and Cardillo, G. Oxidation of Alcohols, Chromium Oxidations in Organic Chemistry, Springer-Verlag, Berlin, pages 118-216, 1984.

- [6] Mancuso, A. J. and Swern, D. Activated dimethyl sulfoxide: Useful reagents for synthesis. *Synthesis*, 1981(03): 165-185, 1981.
- [7] Ishii, Y., Yamawaki, K., Ura, T., Yamada, H., Yoshida, T., and Ogawa, M. Hydrogen peroxide oxidation catalyzed by heteropoly acids combined with cetylpyridinium chloride. Epoxidation of olefins and allylic alcohols, ketonization of alcohols and diols, and oxidative cleavage of 1, 2-diols and olefins. *The Journal of Organic Chemistry*, 53(15): 3587-3593, 1988.
- [8] Jia, A., Lou, L. L., Zhang, C., Zhang, Y., and Liu, S. Selective oxidation of benzyl alcohol to benzaldehyde with hydrogen peroxide over alkali-treated ZSM-5 zeolite catalysts. *Journal of Molecular Catalysis A: Chemical*, 306(1-2): 123-129, 2009.
- [9] Ammam, M. Polyoxometalates: Formation, structures, principal properties, main deposition methods and application in sensing. *Journal of Materials Chemistry A*, 1(21): 6291-6312, 2013.
- [10] Long, D. L., Burkholder, E., and Cronin, L. Polyoxometalate clusters, nanostructures and materials: From self assembly to designer materials and devices. *Chemical Society Reviews*, 36(1): 105-121, 2007.
- [11] Khan, M. I. Novel extended solids composed of transition metal oxide clusters. *Journal of Solid State Chemistry*, 152(1): 105-112, 2000.
- [12] Long, D. L. and Cronin, L. Towards polyoxometalate-integrated nanosystems. *Chemistry—A European Journal*, 12(14): 3698-3706, 2006.
- [13] Rhule, J. T., Hill, C. L., Judd, D. A., and Schinazi, R. F. Polyoxometalates in medicine. *Chemical Reviews*, 98(1): 327-358, 1998.
- [14] Nomiya, K., Torii, H., Hasegawa, T., Nemoto, Y., Nomura, K., Hashino, K., Uchida, M., Kato, Y., Shimizu, K., and Oda, M. Insulin mimetic effect of a tungstate cluster. Effect of oral administration of homo-polyoxotungstates and vanadium-substituted polyoxotungstates on blood glucose level of STZ mice. *Journal of Inorganic Biochemistry*, 86(4): 657-667, 2001.
- [15] Ma, H., Peng, J., Han, Z., Yu, X., and Dong, B. A novel biological active multilayer film based on polyoxometalate with pendant support-ligand. *Journal of Solid State Chemistry*, 178(12): 3735-3739, 2005.
- [16] Errington, R. J., Petkar, S. S., Horrocks, B. R., Houlton, A., Lie, L. H., and Patole, S. N. Covalent immobilization of a  $TiW_5$  polyoxometalate on derivatized silicon surfaces. *Angewandte Chemie*, 117(8): 1280-1283, 2005.

- [17] Witte, P. T., Chowdhury, S. R., ten Elshof, J. E., Sloboda-Rozner, D., Neumann, R., and Alsters, P. L. Highly efficient recycling of a “sandwich” type polyoxometalate oxidation catalyst using solvent resistant nanofiltration. *Chemical Communications*, (9): 1206-1208, 2005.
- [18] Neumann, R., Khenkin, A. M., and Vigdergauz, I. Quinones as co-catalysts and models for the surface of active carbon in the phosphovanadomolybdate-catalyzed aerobic oxidation of benzylic and allylic alcohols: Synthetic, kinetic, and mechanistic aspects. *Chemistry—A European Journal*, 6(5): 875-882, 2000.
- [19] Liu, S., Volkmer, D., and Kurth, D.G. Smart polyoxometalate-based nitrogen monoxide sensors. *Analytical chemistry*, 76(15): 4579-4582, 2004.
- [20] Coronado, E., Giménez-Saiz, C., and Gómez-García, C. J. Recent advances in polyoxometalate-containing molecular conductors. *Coordination Chemistry Reviews*, 249(17-18): 1776-1796, 2005.
- [21] Patel, A. and Pathan, S. Solvent free selective oxidation of styrene and benzyl alcohol to benzaldehyde over an eco-friendly and reusable catalyst, undecamolybdophosphate supported onto neutral alumina. *Industrial & Engineering Chemistry Research*, 51(2): 732-740, 2012.
- [22] Peng, G., Wang, Y., Hu, C., Wang, E., Feng, S., Zhou, Y., Ding, H. and Liu, Y. Heteropolyoxometalates which are included in microporous silica,  $Cs_xH_{3-x}PMo_{12}O_{40}/SiO_2$  and  $Cs_yH_{5-y}PMo_{10}V_2O_{40}/SiO_2$ , as insoluble solid bifunctional catalysts: synthesis and selective oxidation of benzyl alcohol in liquid–solid systems. *Applied Catalysis A: General*, 218(1-2):91-99, 2001.
- [23] Kholdeeva, O. A., Maksimchuk, N. V., and Maksimov, G. M.. Polyoxometalate-based heterogeneous catalysts for liquid phase selective oxidations: Comparison of different strategies. *Catalysis Today*, 157(1-4):107-113, 2010.
- [24] Zhang, R., Ding, W., Tu, B., and Zhao, D. Mesoporous Silica: An efficient nanoreactor for liquid–liquid biphasic reactions. *Chemistry of Materials*, 19(18): 4379-4381, 2007.
- [25] Dengel, A. C., Griffith, W. P., and Parkin, B. C. Studies on polyoxo- and polyperoxo-metalates. Part 1. Tetrameric heteropolyperoxotungstates and heteropolyperoxomolybdates. *Journal of the Chemical Society, Dalton Transactions*, (18): 2683-2688, 1993.
- [26] Bortolini, O., Campestrini, S., Di Furia, F., Modena, G., and Valle, G. Metal catalysis in oxidation by peroxides. 27. Anionic molybdenum-picolinate N-oxido-

- peroxo complex: An effective oxidant of primary and secondary alcohols in nonpolar solvents. *The Journal of Organic Chemistry*, 52(24): 5467-5469, 1987.
- [27] Ingle, R. H., Vinu, A., and Halligudi, S. B. Alkene epoxidation catalyzed by vanadomolybdophosphoric acids supported on hydrated titania. *Catalysis Communications*, 9(5): 931-938, 2008.
- [28] Katsoulis, D. E. A survey of applications of polyoxometalates. *Chemical Reviews*, 98(1): 359-388, 1998.
- [29] Zhang, Q., Zhang, S., and Deng, Y. Recent advances in ionic liquid catalysis. *Green Chemistry*, 13(10): 2619-2637, 2011.
- [30] Zhou, Y., Guo, Z., Hou, W., Wang, Q., and Wang, J., 2015. Polyoxometalate-based phase transfer catalysis for liquid–solid organic reactions: A review. *Catalysis Science & Technology*, 5(9): 4324-4335.
- [31] Davis, Jr, J. H. Task-specific ionic liquids. *Chemistry Letters*, 33(9): 1072-1077, 2004.
- [32] Cole, A. C., Jensen, J. L., Ntai, I., Tran, K. L. T., Weaver, K. J., Forbes, D. C., and Davis, J. H. Novel Brønsted acidic ionic liquids and their use as dual solvent–catalysts. *Journal of the American Chemical Society*, 124(21): 5962-5963, 2002.
- [33] Bates, E. D., Mayton, R. D., Ntai, I., and Davis, J. H. CO<sub>2</sub> capture by a task-specific ionic liquid. *Journal of the American Chemical Society*, 124(6): 926-927, 2002.
- [34] Hajipour, A. R. and Rafiee, F. Basic ionic liquids. A short review. *Journal of the Iranian Chemical Society*, 6: 647-678, 2009.
- [35] Nadealian, Z., Mirkhani, V., Yadollahi, B., Moghadam, M., Tangestaninejad, S., and Mohammadpoor-Baltork, I. Selective oxidation of alcohols to aldehydes using inorganic–organic hybrid catalyst based on zinc substituted polyoxometalate and ionic liquid. *Journal of Coordination Chemistry*, 65(6):1071-1081, 2012.
- [36] Chen, G., Zhou, Y., Long, Z., Wang, X., Li, J., and Wang, J. Mesoporous polyoxometalate-based ionic hybrid as a triphasic catalyst for oxidation of benzyl alcohol with H<sub>2</sub>O<sub>2</sub> on water. *ACS Applied Materials & Interfaces*, 6(6): 4438-4446, 2014.
- [37] Zhou, Y., Chen, G., Long, Z., and Wang, J. Recent advances in polyoxometalate-based heterogeneous catalytic materials for liquid-phase organic transformations. *RSC Advances*, 4(79): 42092-42113, 2014.

- [38] Leng, Y., Liu, J., Jiang, P., and Wang, J. Heteropolyanion-based polymeric hybrids: Highly efficient and recyclable catalysts for oxidation of alcohols with H<sub>2</sub>O<sub>2</sub>. *RSC Advances*, 2(31): 11653-11656, 2012.
- [39] Qiao, Y., Hou, Z., Li, H., Hu, Y., Feng, B., Wang, X., Hua, L., and Huang, Q. Polyoxometalate-based protic alkylimidazolium salts as reaction-induced phase-separation catalysts for olefin epoxidation. *Green Chemistry*, 11(12): 1955-1960, 2009.
- [40] Keshavarz, M., Iravani, N., and Parhami, A. Novel SO<sub>3</sub>H-functionalized polyoxometalate-based ionic liquids as highly efficient catalysts for esterification reaction. *Journal of Molecular Structure*, 1189: 272-278, 2019.
- [41] Saikia, S. and Borah, R. 2-Methyl-1, 3-disulfoimidazolium polyoxometalate hybrid catalytic systems as equivalent safer alternatives to concentrated sulfuric acid in nitration of aromatic compounds. *Applied Organometallic Chemistry*, 33(10): e5146, 2019.
- [42] Bridgeman, A. J. Density functional study of the vibrational frequencies of  $\alpha$ -Keggin heteropolyanions. *Chemical Physics*, 287(1-2): 55-69, 2003.
- [43] Mioč, U., Colomban, P., and Novak, A. Infrared and Raman study of some heteropolyacid hydrates. *Journal of Molecular Structure*, 218: 123-128, 1990.
- [44] Rocchiccioli-Deltcheff, C., Fournier, M., Franck, R., and Thouvenot, R. Vibrational investigations of polyoxometalates. 2. Evidence for anion-anion interactions in molybdenum (VI) and tungsten (VI) compounds related to the Keggin structure. *Inorganic Chemistry*, 22(2): 207-216, 1983.
- [45] Rao, G. R. and Rajkumar, T. Interaction of Keggin anions of 12-tungstophosphoric acid with Ce<sub>x</sub>Zr<sub>1-x</sub>O<sub>2</sub> solid solutions. *Journal of Colloid and Interface Science*, 324(1-2): 134-141, 2008.
- [46] Rajkumar, T. and Ranga Rao, G. Investigation of hybrid molecular material prepared by ionic liquid and polyoxometalate anion. *Journal of Chemical Sciences*, 120: 587-594, 2008.
- [47] de Oliveira Jr, M., Rodrigues-Filho, U. P., and Schneider, J. Thermal transformations and proton species in 12-phosphotungstic acid hexahydrate studied by <sup>1</sup>H and <sup>31</sup>P solid-state nuclear magnetic resonance. *The Journal of Physical Chemistry C*, 118(22): 11573-11583, 2014.
- [48] Ganapathy, S., Fournier, M., Paul, J. F., Delevoye, L., Guelton, M., and Amoureux, J. P. Location of protons in anhydrous Keggin heteropolyacids H<sub>3</sub>PMo<sub>12</sub>O<sub>40</sub> and

- H<sub>3</sub>PW<sub>12</sub>O<sub>40</sub> by <sup>1</sup>H {<sup>31</sup>P}/<sup>31</sup>P {<sup>1</sup>H} REDOR NMR and DFT quantum chemical calculations. *Journal of the American Chemical Society*, 124(26): 7821-7828, 2002.
- [49] Li, Z., Zhang, Q., Liu, H., He, P., Xu, X., and Li, J. Organic–inorganic composites based on room temperature ionic liquid and 12-phosphotungstic acid salt with high assistant catalysis and proton conductivity. *Journal of Power Sources*, 158(1): 103-109, 2006.
- [50] Leng, Y., Wang, J., Zhu, D., Shen, L., Zhao, P., and Zhang, M. Heteropolyanion-based ionic hybrid solid: A green bulk-type catalyst for hydroxylation of benzene with hydrogen peroxide. *Chemical Engineering Journal*, 173(2): 620-626, 2011.
- [51] Zhao, P., Zhang, M., Wu, Y., and Wang, J. Heterogeneous selective oxidation of sulfides with H<sub>2</sub>O<sub>2</sub> catalyzed by ionic liquid-based polyoxometalate salts. *Industrial & Engineering Chemistry Research*, 51(19): 6641-6647, 2012.
- [52] Bridgeman, A. J. Computational study of the vibrational spectra of α- and β-Keggin polyoxometalates. *Chemistry—A European Journal*, 10(12): 2935-2941, 2004.
- [53] Ranga Rao, G. and Rajkumar, T. Investigation of 12-tungstophosphoric acid supported on Ce<sub>0.5</sub>Zr<sub>0.5</sub>O<sub>2</sub> solid solution. *Catalysis Letters*, 120: 261-273, 2008.
- [54] Rao, G. R., Rajkumar, T., and Varghese, B. Synthesis and characterization of 1-butyl 3-methyl imidazolium phosphomolybdate molecular salt. *Solid State Sciences*, 11(1): 36-42, 2009.
- [55] Ding, Y., Gao, Q., Li, G., Zhang, H., Wang, J., Yan, L., and Suo, J.. Selective epoxidation of cyclohexene to cyclohexene oxide catalyzed by Keggin-type heteropoly compounds using anhydrous urea–hydrogen peroxide as oxidizing reagent and acetonitrile as the solvent. *Journal of Molecular Catalysis A: Chemical*, 218(2): 161-170, 2004.
- [56] Venturello, C. and D'Aloisio, R. Quaternary ammonium tetrakis (diperoxotungsto) phosphates (3-) as a new class of catalysts for efficient alkene epoxidation with hydrogen peroxide. *The Journal of Organic Chemistry*, 53(7): 1553-1557, 1988.
- [57] Duncan, D. C., Chambers, R. C., Hecht, E., and Hill, C. L. Mechanism and dynamics in the H<sub>3</sub>[PW<sub>12</sub>O<sub>40</sub>]-catalyzed selective epoxidation of terminal olefins by H<sub>2</sub>O<sub>2</sub>. Formation, reactivity, and stability of {PO<sub>4</sub>[WO(O<sub>2</sub>)<sub>2</sub>]<sub>4</sub>}<sup>3-</sup>. *Journal of the American Chemical Society*, 117(2): 681-691, 1995.
- [58] Das, N., Chowdhury, S., and Purkayastha, R. N. D. Peroxo–tungstate (VI) complexes: Syntheses, characterization, reactivity, and DFT studies. *Monatshefte für Chemie-Chemical Monthly*, 150: 1255-1266, 2019.

- [59] Dengel, A. C., Griffith, W. P., Powell, R. D., and Skapski, A. C. Studies on transition-metal peroxo complexes. Part 7. Molybdenum (VI) and tungsten (VI) carboxylato peroxo complexes, and the X-ray crystal structure of  $K_2[MoO(O_2)_2(glyc)] \cdot 2H_2O$ . *Journal of the Chemical Society, Dalton Transactions*, (5): 991-995, 1987.
- [60] Dutta, A. K., Gogoi, P., and Borah, R. Diethyldisulfoammonium chlorometallates as heterogeneous Brønsted–Lewis acidic catalysts for one-pot synthesis of 14-aryl-7-(N-phenyl)-14H-dibenzo[a,j] acridines. *Applied Organometallic Chemistry*, 32(1): e3900, 2018.